수의학 석사학위 논문

신경세포에서 당질코르티코이드 유도성 미토콘드리아 기능 장애에 대한 멜라토닌의 방어 효과

The protective effect of melatonin on glucocorticoid-induced mitochondrial dysfunction in neuronal cells

2023년 2월

서울대학교 대학원

수의학과 수의생명과학 전공

김 민 정

신경세포에서 당질코르티코이드 유도성 미토콘드리아 기능 장애에 대한 멜라토닌의 방어 효과

The protective effect of melatonin on glucocorticoid-induced mitochondrial dysfunction in neuronal cells

지도교수 한 호 재

이 논문을 수의학 석사 학위논문으로 제출함

2022년 11월

서울대학교 대학원

수의학과 수의생명과학 전공

김민정

김민정의 수의학 석사 학위논문을 인준함

2023년 1월

위 원 장 _____ 이 장 헌 _____ (인)

부위원장 _____ 한 호 재 _____ (인)

위 원 _____ 이 현 직 _____ (인)

ABSTRACT

The protective effect of melatonin on glucocorticoid-induced mitochondrial dysfunction in neuronal cells

Min Jeong Kim
Major in Veterinary Biomedical Science
Department of Veterinary Medicine
The Graduate School
Seoul National University

Glucocorticoid and melatonin are hormones that maintain neural homeostasis by regulating circadian rhythms. However, high levels of glucocorticoid trigger mitochondrial dysfunction including defective mitophagy by increasing the activity of glucocorticoid receptors (GRs). Melatonin then suppresses glucocorticoid-induced stress-responsive neurodegeneration. Therefore, the study

investigated how melatonin regulates chaperone proteins related to GR trafficking into the nucleus to suppress glucocorticoid action. In this study, the effects of glucocorticoid on mitochondrial dysfunction, neuronal cell apoptosis, and cognitive deficits were reversed by melatonin treatment. Then, melatonin inhibits the nuclear translocation of GRs in both SH-SY5Y cells and mouse hippocampal tissue. Moreover, melatonin selectively suppressed the expression of FKBP prolyl isomerase 4 (FKBP4) to reduce the nuclear translocation of GRs among the chaperone proteins and nuclear trafficking proteins. In both cells and hippocampal tissue, melatonin up-regulated melatonin receptor 1 (MT1) bound to $G\alpha q$, which triggered the phosphorylation of ERK1. The activated ERK then enhanced DNA methyltransferase 1 (DNMT1)-mediated hypermethylation of the *FKBP52* promoter. By knocking down DNMT1, GR-mediated mitochondrial dysfunction and cell apoptosis were reduced. In conclusion, melatonin has a protective effect against glucocorticoid-induced defective mitophagy and neurodegeneration by FKBP4 down-regulation that reduced the nuclear translocation of GRs.

Keywords: Melatonin, Glucocorticoid, Glucocorticoid receptor, Mitophagy, Apoptosis, FKBP4
Student Number: 2020-27673

CONTENTS

LIST OF FIGURES

ABBREVIATIONS

5-aza	5-Azacytidine
5-mc	5-Methylcytosine
AD	Alzheimer's disease
BNIP3L	BCL-2/adenovirus E1B 19kda protein-interacting protein 3-like
CCCP	Carbonyl cyanide m-chlorophenyl hydrazone
DNMT	DNA methyltransferase
ELISA	Enzyme-linked immunosorbent assay
FBS	Fetal bovine serum
FKBP	FKBP prolyl isomerase
gDNA	Genomic DNA
GR	Glucocorticoid receptor
HDAC	Histone deacetylase
hDPCs	Human dental pulp cells
HPA axis	Hypothalamic-pituitary-adrenal axis
HSP90	Heat shock protein 90

IACUC	Institutional animal care and use committee
ICC	Immunocytochemistry
IHC	Immunohistochemistry
MSP	Methylation specific PCR
MT	Melatonin receptor
MTG	Mitotracker green
mtROS	Mitochondrial ROS
MQC	Mitochondrial quality control system
NPC	Nuclear pore complex
NT	Non-targeting
NUP	Nuclear pore glycoprotein
PLA	Proximity ligation assay
S.E.M.	Standard error of mean
siRNAs	Small interfering RNAs
SRRF	Super-resolution radial fluctuations
TMRE	Tetramethylrhodamine ethyl ester

INTRODUCTION

Stress-induced high levels of glucocorticoid can cause mitochondrial dysfunction, a major early pathological feature of numerous neurodegenerative diseases, by impairing the mitochondrial quality control system, such as mitophagy (Choi & Han, 2021; Schmidt et al., 2004). Under stress conditions, glucocorticoid-bound GRs move from the cytosol to the nucleus, triggering stress response signaling pathways such as promoting apoptosis or depression-related gene expression acting as a transcription factor or a co-factor (Aziz et al., 2012; Cattaneo & Riva, 2016; Clarisse et al., 2020; Scheschowitsch et al., 2017). According to previous research, activated GRs by excessive glucocorticoid directly binds to the PGC1α promoter as a transrepressor, reducing its expression and nuclear translocation, which resulted in downregulation of NIX. NIX, otherwise known as BCL-2/adenovirus E1B 19kda protein-interacting protein 3-like (BNIP3L), is located on the outer membrane of mitochondria acting as a mitophagy receptor interacting with LC3/GABARAP protein

and induces clearance of damaged or dysfunctional mitochondria forming mitophagosome. Also, NIX is capable of maintaining basal mitophagy that continuously occurs mostly in energy-demanding tissues such as heart and brain and compensating for other regulators of mitophagy (McWilliams et al., 2018). Especially, we previously found that glucocorticoid inhibits NIX-dependent mitophagy but does not trigger the PINK1-parkin pathway which is not able to compensate for the reduced basal mitophagy (Choi et al., 2021). For these reasons, finding a strategy to reduce the nuclear translocation of GRs is thereby important to suppress mitochondrial dysfunction induced by glucocorticoid-induced NIX deficiency. Without a ligand, GR in the cytosolic compartment forms a multiprotein complex with chaperones and co-chaperone proteins including heat shock protein90 (HSP90), FKBP51 (FKBP5), FKBP52 (FKBP4), PP5, and CyP90, most of which contribute to the retention of GR in the cytosol (Kaziales et al., 2020; Pratt et al., 2006; Zgajnar et al., 2019). However, ligand-bound GRs disassociate from chaperones and move into the nucleus along the microtubule with the help of some co-chaperone proteins, dynein motor proteins, and nuclear pore complex (NPC) including importins (Echeverría et al., 2009; Vandevyver et al., 2012). Accordingly, finding the molecules that regulate chaperone proteins and then

inhibiting GR nuclear translocation would prevent glucocorticoid-induced defects in NIX-mediated mitophagy and neuronal cell survival.

Like glucocorticoids, melatonin is a major circadian hormone that regulates sleep, mood, and appetite (Chen et al., 2017; Chojnacki et al., 2015; Kruk et al., 2021). During stress, the pineal gland, which produces melatonin, is a target site of glucocorticoid-mediated damage because it also expresses a high density of GRs as other regions such as the hippocampus or prefrontal cortex that mainly regulate stress response (Bob & Fedor-Freybergh, 2008; Couto-Moraes et al., 2009; Dagnino-Subiabre et al., 2006). High levels of glucocorticoid reduce melatonin release from the pineal gland by down-regulating NF-κB. Accordingly, its beneficial functions such as enhancing mitochondrial health and protecting against neurodegenerative diseases are inhibited (Boga et al., 2019; da Silveira Cruz-Machado et al., 2017; Luo et al., 2020). Thus, restoring melatonin can prevent glucocorticoid-induced mitochondrial defects and neurodegenerative diseases. In addition to the antioxidant function of melatonin, it can inhibit glucocorticoid actions by suppressing GR activity or expression (Quiros et al., 2008). For example, melatonin-impaired GR-HSP90 interaction suppresses GR nuclear translocation (Presman et al., 2006).

Moreover, melatonin is associated with changes in the density and affinity of the cytoplasmic and nuclear conformation of GRs in rats, but whether melatonin increases or decreases these changes is different depending on the tissue (Hoijman et al., 2004). These findings suggest that protective mechanism of melatonin on mitochondria shows high dependence on glucocorticoid-mediated pathways. Therefore, I assume that melatonin can highly affect proteins involved with GR activity or expression, thus blocking glucocorticoid-mediated pathways.

In the present study, human neuroblastoma SH-SY5Y cells, a widely used *in vitro* model to investigate neurodegeneration, were used to explore the detailed regulatory mechanism of nuclear transport of GR by melatonin. In addition, ICR mice mimicking a stress-induced model were used as an *in vivo* model to determine the restorative effects of melatonin on mitochondrial dysfunction and cognitive impairment induced by high doses of corticosterone. Therefore, this study used both *in vitro* and *in vivo* models to investigate the protective mechanisms of melatonin on stress-induced mitochondria dysfunction and cognitive impairment.

MATERIALS AND METHODS

1. Materials

The neuroblastoma cell line SH-SY5Y was purchased from Korea Cell Line Bank (Seoul, Korea). Fetal bovine serum (FBS) was purchased from Hyclone (Logan, UT, USA) and antibiotics were purchased from Gibco (Grand Island, NY, USA). Small interfering RNAs (siRNAs) for *FKBP52*, *MT1*, *DNMT1* and non-targeting (NT) were purchased from Bioneer (Daejeon, Korea). Cortisol, corticosterone, BSA, DAPI, α-tubulin antibody (T6074), melatonin (M5250), PD98059 (027K2176), 5-azacytidine (5-aza, A2385) and carbonyl cyanide m-chlorophenyl hydrazone (CCCP, C2759) were purchased from Sigma Chemical Company (St. Louis, MO, USA). Lamin A/C (sc-376248), β-actin (sc-47778), MT2 (sc-28453), dynein (sc-13524), NUP62 (sc-48373), importin β (sc-

137016), BNIP3 (sc-56167), c-MYC (sc-40), IgG mouse (sc-2025), p-ERK (sc-7383), ERK (sc-94), JNK (sc-7345), p-JNK (sc-6254), p-p38 (sc-166182), and PINK1 (sc-33796) antibodies were acquired from Santa Cruz (Paso Robles, CA, USA). MT1 (NBP1-71113), FKBP4 (NB110-96874), FKBP5 (NBP1-84676), LC3 (NB100-2220) and NIX (NBP1-88558) were purchased from Novus Biologicals (Littleton, CO, USA). TOMM20 (ab56783), p-GR (ab55189), DNMT1 (ab19905), DNMT3a (ab23565), and SP1 (ab227383) antibodies were obtained from Abcam (Cambridge, MA, USA). Cleaved caspase 3 (9661S), DNMT3b (67259S), GR (12041S), 5-methylcytosine (5-mc, 28692S), p38 (9212S), IgG rabbit (2729S), and p-c-MYC ser62 (13748S) antibodies were purchased from Cell Signaling Technology (Danvers, MA, USA). HSP90 antibody (PA3-013) was obtained from Thermo Fisher (Rockford, IL, USA). Melatonin ELISA kit (MBS765748) was purchased from MyBioSource company (San Diego, CA, USA). EZ DNA Methylation-Lightning Kit (D5030) was purchased from Kyongshin Scientific company (Seoul, Korea)

2. Experimental design of the animal study

Male ICR mice aged 7 weeks were used, in compliance and approval with the Institutional Animal Care and Use Committee (IACUC) of Seoul National University (SNU-211027-5). All experiments of this study were conducted according to IACUC guidelines. ICR mice were delivered from Orient-Bio (Seoul, Korea). After measuring the weight of each mouse, mice were randomly divided into four groups of the same size, including the control group, the corticosterone-treated group, the corticosterone and melatonin-treated group, and the melatonin-treated group. They were housed for 7 days in controlled specific pathogen-free conditions of 22 ℃, 70% relative humidity, a 12 h light: dark cycle, and had unlimited access to a normal diet and water. The mice of corticosterone-treated group were administered 10 mg/kg of corticosterone and the melatonin-treated group was intraperitoneally administered at 10 mg/kg of melatonin for 7 days. The mice of the corticosterone and the melatonin-treated group were firstly administered 10 mg/kg of melatonin and then given 10 mg/kg of corticosterone 30 min later intraperitoneally for 7 days. After behavioral testing, mice were anesthetized by intraperitoneal injection of alfaxalone (40

mg/kg) with 10 mg/kg xylazine and sacrificed for acquiring brain tissue samples.

3. Y-maze spontaneous alternation test

The Y-maze behavioral test is used to evaluate spatial memory and learning. Mice instinctively prefer to try a new arm of the Y-maze instead of returning to the one they've already explored. Before the Y-maze spontaneous alternation test, the mice were accommodated in the testing room for 2 h to reduce the effects of external environmental stimuli or unintentional stress on their behavior. First, mice were positioned in the Y-maze apparatus. For 8 min, mice were allowed to explore the Y-maze, and the movements of the mice were recorded by using a video camera. The number of alternations was divided by the number of total triads. Animals with a higher alternation percentage tend to have better spatial memory.

4. Novel object recognition test

The novel object recognition test is a commonly used mouse behavioral test for assessing object working memory. The mice were habituated for 5 min in an open-field box. After 24 h, the mice were allowed to move freely in the same open field with two comparable items for 10 min. After 4 h, one of the two objects was replaced with a new one, then the mouse was given 10 min to explore the open field. The discrimination index is the most used value for cognitive evaluation.

5. Immunocytochemistry (ICC)

Cultured cells were fixed with 4% paraformaldehyde for 10 min at room temperature and then incubated in 0.1% Triton X for 5 min. To inhibit the nonspecific binding of antibodies, cells were incubated with 5% normal goat serum for 1h. Next, the cells were treated with primary antibody for 24 h at 4 ℃. After being washed with PBS, the cells were applied for 2 h at room temperature with Alexa Fluor

488 or 555-conjugated secondary antibody (1:300) in dark for 2 h at room temperature. Images were acquired by super-resolution radial fluctuations (SRRF) imaging system (Andor Technology, Belfast, UK). The fluorescent intensity analysis and co-localization were performed with Fiji software (developed by Wayne Rasband, National Institutes of Health, Bethesda, MD, USA)

6. Immunohistochemistry (IHC)

Mice were deeply anesthetized and transcardially perfused with PBS, and then with 4% paraformaldehyde in 0.1 M phosphate buffer (pH 7.4). The extracted brains were post-fixed for 2 h in 4% paraformaldehyde and then dehydrated in 30% sucrose in PBS for 24 h at 4 ℃. Serial transverse sections (40㎛) were conducted using a cryostat (Leica Biosystems, Nussloch, Germany). The brain tissues were fixed with 4% paraformaldehyde and blocked with 5% normal goat serum containing 0.1% Triton X-100 for 1 h at room temperature. Brain samples were incubated with primary antibody overnight at 4 ℃. Then, the secondary antibody was incubated for 2 h at room temperature. All completed samples were visualized using the SRRF imaging system. Fiji software was used to analyze the

fluorescent intensity and determine Pearson ' s correlation coefficient values.

7. Cell culture

The human neuroblastoma cell line SH-SY5Y was cultured in high-glucose DMEM supplemented with 10% FBS and 1% antibiotics. Cells were grown in 60 mm dishes and 100 mm culture dishes in an incubator (37 ℃, CO_2 5%, and air 95%). When the cells reached 70% confluency, the culture medium was replaced with a serum-free medium containing 1% antibiotics for 24 h for starvation.

8. Real time PCR

RNA was extracted from SH-SY5Y using an RNA extraction Kit (TaKaRa, Otsu, Shinga, Japan, 9767). Reverse transcription PCR was performed using 1 μg of extracted RNA using a Maxime RT-PCR premix kit (iNtRON Biotechnology, Sungnam, Korea, 25801). The cDNA was amplified using a Rotor-Gene 6000 real-time system (Corbett Research, Mortlake, Australia) using a variety of

PCR primers were created according to the sequence below

mRNA primers (Table 1) and TB^{TM} Green Premix EX Taq^{TM} (TaKaRa, RR420A). The real time PCR was conducted as follows: 10 min at 95 ℃, 15 s at 58 ℃, and 20 s at 72 ℃. To quantify mRNA expression, delta delta Ct method was used and the data were normalized to the *ACTB* gene.

PCR primers were created according to the sequence below

Table 1. PCR primer

Target gene	Sequence (forward)	Sequence (reverse)
NIX	GGA CTC GGC TTG TTG TGT TG	TAG CTC CAC CCA GGA ACT GT
PPP5C	CCC AAC TAC TGC GAC CAG AT	CCC GTC ACC TCA CAT CAT TC
PTGES	CTT CCT TTT CCT GGG CTT CG	GAA GAC CAG GAA GTG CAT CCA
HSP90	GTA AGC GAT GAT GAG GCT GA	GTC CAG ATG GGC TTT GTT TT
FKBP51	CTG GAA GTA AAC CCC CAG AA	TGC TTT ATT GGC CTC TTC CT
FKBP52	GAA TAC AGA CTC GCG GTG AA	CCA TAA GGC AGA TCC AGG TT
GR	TGG TGT CAC TGT TGG AGG TT	AAA CCT GGT ATT GCC TTT GC
DYNC1N1	GCC ACC GTC AGT TTT GAC AC	AAA TTG CCT CCA CCA AAC GC
DYCN1	CGG AAC CTG AAT CTG GAA GAG	TGC AGC TCA TCG TTC ATC TC
DYCN2	GTG AAG GAG TCA GCC ACA GA	GCT GTT CTT TGT TGC TTC CA
NUP62	ACA TCG ATG CAC AGC TCA AG	ACT GCA GTG AGT CCA TGT GC
KPNB	ACC TGC CCA CTT TCC TTG TG	CTC TGC TGA TAT TGT GCC TTG A
DNMT1	TGA GGC CTT CAC GTT CAA CA	TCC AGG TTG CTG CCT TTG AT
DNMT3a	TGC CGG AAC ATT GAG GAC AT	TGG CAC ATT CCT CCA ACG AA
DNMT3b	ACG TCG CTT CTG AAG TGT GT	TCC GCC AAT CAC CAA GTC AA

HDAC1	CGA TCT GCT CCT CTG ACA AA	CCT TGG TTT TCT CCT CTT CG
HDAC2	ACT GCC GAA GAA ATG ACA AA	CAC CAC TGT TGT CCT TGG AT
HDAC3	GGC TTC TGC TAT GTC AAC GA	TCC GTA TTT GTG GAA GGA CA
HDAC8	GCG TGT TTA TGC AAG CAG TT	TTC CCC TAG GTC CAG TTG AG

9. Western blotting

Cells were collected with RIPA lysis buffer (ATTO Corporation, Tokyo, Japan, WSE-7420) containing protease and phosphatase inhibitor (Thermo Fisher, 78440) and incubated on ice. After homogenization, cell lysates were centrifuged at 13,000 rpm for 20 min. The protein concentration was determined by a BCA assay kit (Thermo Fisher, 23227). The same amount of sample was loaded in an 8-15% SDS-polyacrylamide gel for electrophoresis and then transferred to a polyvinylidene fluoride membrane. The membrane was blocked with 5% skim milk (Gibco, 232100) for 40 min, and blocked membrane was washed with TBST solution 3 times every 10 min. Next, the membrane was incubated with primary antibody overnight at 4 ℃. After incubation, the membrane was washed with TBST solution 3 times every 10 min and incubated with horseradish peroxidase-conjugated secondary antibody (1:10,000) at room temperature for 2 h. The western blotting bands were detected by

using chemiluminescence (BioRad, Hercules, CA, USA). The quantification of protein bands was performed using the Image J program (developed by Wayne Rasband, National Institutes of Health, Bethesda, MD, USA).

10. Subcellular fractionation

Subcellular fractionation was conducted using the EzSubcell subcellular fractionation/extraction kit (ATTO Corporation, WSE-7421) to isolate cytosolic and nuclear proteins. Cytosolic and nuclear samples for western blot analysis were prepared according to the manufacturer's manual. Lamin A/C and α-tubulin were used as a nuclear and cytosolic protein marker, respectively.

11. siRNA transfection

Cells were grown until approximately 70% confluency of the plate. Before treating cortisol and melatonin, cells were incubated with a mixture of 25 nM indicated siRNA and transfection reagent TurboFect (Thermo Fisher, R0531) for 24 h without antibiotics.

The medium was changed to serum-free high glucose DMEM. NT siRNA was used as the negative control.

12. Measurement of intracellular ROS, mitochondrial ROS (mtROS) and mitochondrial membrane potential

CM-H_2DCFDA, MitoSOX™ (Thermo Fisher, M36008), and tetramethylrhodamine ethyl ester (TMRE, Sigma Chemical Company, 87917) were used to determine intracellular ROS, mtROS, and mitochondrial membrane potential, respectively. Cells were washed once with PBS and incubated with 1 μM CM-H2DCFDA for 15 min, 5 μM MitoSOX™ for 15 min at 37 ℃, and 100 nM TMRE for 20 min at 37 ℃ in dark. Then, cells were treated with 0.05% trypsin for 3 min and centrifuged at 1,500 g for 5 min. Harvested cells were suspended in 400 μL PBS. Fluorescence intensities of CM-H2DCFDA, MitoSOX™, and TMRE were detected by using a Cytoflex flow cytometer (CytoFlex; Beckman Coulter, USA).

13. Measurement of Annexin V/PI apoptosis detection

Annexin V and PI staining were used to detect apoptosis of cells using an annexin V/PI apoptosis detection kit (BD Bioscience, BD 556547). After treatment, cells were suspended in a binding buffer. Next, annexin V-FITC and PI were added to the samples and incubated for 20 min at room temperature in dark. Apoptosis of the samples was detected with flow cytometry (Quanta SC) and data analysis was conducted with CytExpert 2.3 (Beckman Coulter). Annexin V-negative and PI-negative cells were considered viable. Annexin V-negative and PI-positive, Annexin V-positive and PI-positive, Annexin V-positive and PI-negative cells were considered as necrotic, late apoptotic and early apoptotic cells, respectively. Annexin V-positive cells were considered as apoptotic cells.

14. *In situ* proximity ligation assay (PLA)

To identify the interaction between GR and FKBP4, Duolink *in situ*

red starter kit mouse/rabbit (Sigma Chemical Company, #DUO92101) was used. After cell fixation, PLA probe rabbit anti-GR and mouse anti-FKBP4 antibodies were applied. Duolink™ secondary antibodies were applied for 1 h at 37 ℃ and then ligase was added. After adding ligase, amplification was done to amplify the signal. The antibodies ligated together if they were close enough (<40 nm). Fluorescent images were visualized with an SRRF imaging system.

15. Co-immunoprecipitation

Cells were lysed with the pierce™ IP lysis buffer (Thermo Fisher, 87788) containing a protease inhibitor cocktail. Primary antibodies were immobilized with protein G magnetic beads (Sure Beads, BioRad, 161-4021). Immobilized magnetic beads were incubated with cell lysates for overnight at 4 ℃. Beads were washed 3 times with PBST and eluted with 20 mM glycine buffer (pH 2.0) for 5 min. Then, 1 M phosphate buffer and laemmli sample buffer were added to the samples. Protein analysis was conducted by western blot where anti-mouse or rabbit IgG antibody was used as a negative control.

16. Dot blot analysis

Dot blot analysis was used to determine the DNA methylation status of the SH-SY5Y cells. Using a genomic DNA extraction kit, genomic DNA (gDNA) was extracted (Bioneer, K-3032). The 100 ng of extracted gDNA was denatured for 10 min at 95 ℃ and then neutralized on ice for 10 min. On the N^+ nylon membrane (GE Healthcare, Chicago, IL, USA, RPN203B), gDNA was loaded. After drying the membrane, it was incubated at 80 ℃ for 2 h. Then, we used 5% skim milk to block membrane for 1 h. After blocking, it was incubated overnight at 4 ℃ with a 5-mc antibody. The membrane was washed three times with TBST and then incubated for 2 h with HRP-conjugated secondary antibody. To detect DNA, a chemiluminescence detection kit was used (Advansta Inc., K-12045-D50). Image J was used to quantify the dot blot intensity.

17. Chromatin immunoprecipitation (ChIP)

ChIP assay was conducted using an EpiQuik™ chromatin

immunoprecipitation kit (EpiGentek, Farmingdale, NY, USA, P-2002) following the manufacturer's instructions. Samples including protein-chromatin complexes were incubated with ChIP grade antibody, the RNA polymerase (RNAPol), and the normal IgG were used as a positive control and negative control, respectively. Sample DNA was acquired by supplied column and amplified by PCR using a designed primer. SP1 forward primer: CAGAAGGAG GCAAGAACCAA, reverse primer: GTAGGTGGGTCAGGA GCG

18. Methylation specific PCR (MSP)

EZ DNA methylation-lightning kit was used to analyze the methylation of gDNA by bisulfite treatment. MSP was performed to evaluate the methylation status of the *FKBP52* gene in SH-SY5Y cells. MSP was conducted following the manufacturer's instructions (Zymo Research, Irvine, CA, USA, D5030). Methylation status was assessed as a relative level of methylation compared to the unmethylated form. The primer sequences for the CpG site of the *FKBP52* promoter were created according to the sequence below. *FKBP52*-methyl forward primer:

TCGTTATTGTTATTTCGTAGT TTGC, reverse primer: CCTTCTCCTAAAACCCTCGAA, *FKBP52*-unmethyl forward primer: TGTTATTGTTATTTTGTAGTTTGTGT, reverse primer: CCCTTCTCCTAAAACCCTCAA

19. Melatonin enzyme-linked immunosorbent assay (ELISA)

For the quantification of melatonin in mice plasma samples, the melatonin ELISA kit was used. Mice blood was collected in an EDTA tube and centrifuged at 4,000 g for 5 min. All procedures of the melatonin ELISA kit were conducted according to the supplier's protocol.

20. Statistical analysis

Statistical analysis and graphing were performed using GraphPad Prism version 6.0 (GraphPad Inc., San Diego, CA, USA) statistical

software. The sample size ‘n’ represents the number of biological independent replicates. One-way ANOVA (with Dunnett’s multiple comparison test) or two-way ANOVA (with Tukey’s multiple comparison test) were used for analyzing the differences among multiple groups. All quantitative data were expressed as mean±standard error of the mean (S.E.M). A result with a p-value of <0.05 was considered statistically significant.

RESULTS

1. Melatonin-induced improvement in NIX-dependent mitophagy prevents glucocorticoid-induced neuronal cell apoptosis

Glucocorticoid suppresses NIX-mediated mitophagy by increasing the nuclear translocation of GR, which then repressed *PPARGC1A* transcription (Choi et al., 2021). Then, I investigated whether melatonin reversed the suppressive effects of glucocorticoids on mitophagy and the subsequent neurodegeneration. In humans and rodents, major glucocorticoids, such as cortisol and corticosterone, are released during stress. Therefore, SH-SY5Y cells were treated with cortisol and ICR mice with corticosterone. According to a previous study, 1 μM of cortisol was used in SH-SY5Y cells throughout the study, an amount similar to stress-induced levels of glucocorticoids in both humans and rodents (Kirby et al., 2013). To assess the recovering effect of melatonin on mitophagy, mitochondrial contents in SH-SY5Y cells were measured by

detecting mitochondria marker TOMM20 in western blot results and cells stained with mitotracker green (MTG). Melatonin reduced the increased mitochondrial contents by cortisol, representing impaired mitophagy (Fig. 1A and 1B). Then, the extent of mitophagy was detected by immunostaining the cells and hippocampal tissue with LC3 and TOMM20. LC3 bridges mitophagosome components with dysfunctional mitochondria and is converted into LC3II form. My data showed that co-localization between LC3 and TOMM20 was decreased by cortisol and corticosterone, but recovered with melatonin treatment (Fig. 1C and 1D). Next, I confirmed whether melatonin recovered mitophagy by selectively increasing NIX expression. Performing real-time PCR, down-regulated *NIX* mRNA expression by cortisol was significantly recovered by melatonin (Fig. 2A). Consistently, glucocorticoid-induced NIX down-regulation was significantly reversed by melatonin in both SH-SY5Y cells and hippocampal tissue (Fig. 2B and 2C).

Next, I observed whether melatonin recovered cortisol-induced mitochondrial dysfunction and cell apoptosis resulting from impaired NIX-mediated mitophagy. To assess the effect of melatonin on mtROS accumulation and membrane potential, cells were stained with MitoSOX^{TM} and TMRE, which is a cell permeant mitochondrial superoxide indicator and mitochondrial membrane potential,

respectively. Flow cytometry revealed that melatonin reversed cortisol-induced increased mtROS and reduced mitochondrial membrane potential (Fig. 3A and 3B). Mitochondrial dysfunction resulted in cell apoptosis caused by various pathways such as the activation of intrinsic pathways by cytochrome c release. I confirmed that melatonin reduced glucocorticoid-induced cleavage of caspase-3 in both SH-SY5Y cells and hippocampal tissue (Fig. 4A and 4B). Furthermore, the number of annexin V-positive cells, indicating apoptotic cells, was increased following cortisol treatment, whereas melatonin promoted cell survival (Fig. 4C). Then, I determined the recovery effect of melatonin on corticosterone-induced neurodegeneration in mice. In the melatonin ELISA results, melatonin secretion was significantly reduced in mice exposed to excessive corticosterone (Fig. 5A). These results indicated that melatonin restoration can prevent corticosterone-induced neurodegeneration. Neuronal cell death finally triggered behavior changes, especially cognitive deficits when the hippocampus was damaged. Subsequently, the Y-maze alternation test and novel object recognition test were conducted to evaluate spatial and object working memory, respectively. Corticosterone-exposed mice had impaired spatial and object working memory; however, these were restored by melatonin treatment (Fig. 6A and 6B).

Collectively, my results suggested that melatonin recovered glucocorticoid-induced mitochondrial dysfunction, cell death and cognitive impairment by recovering NIX expression.

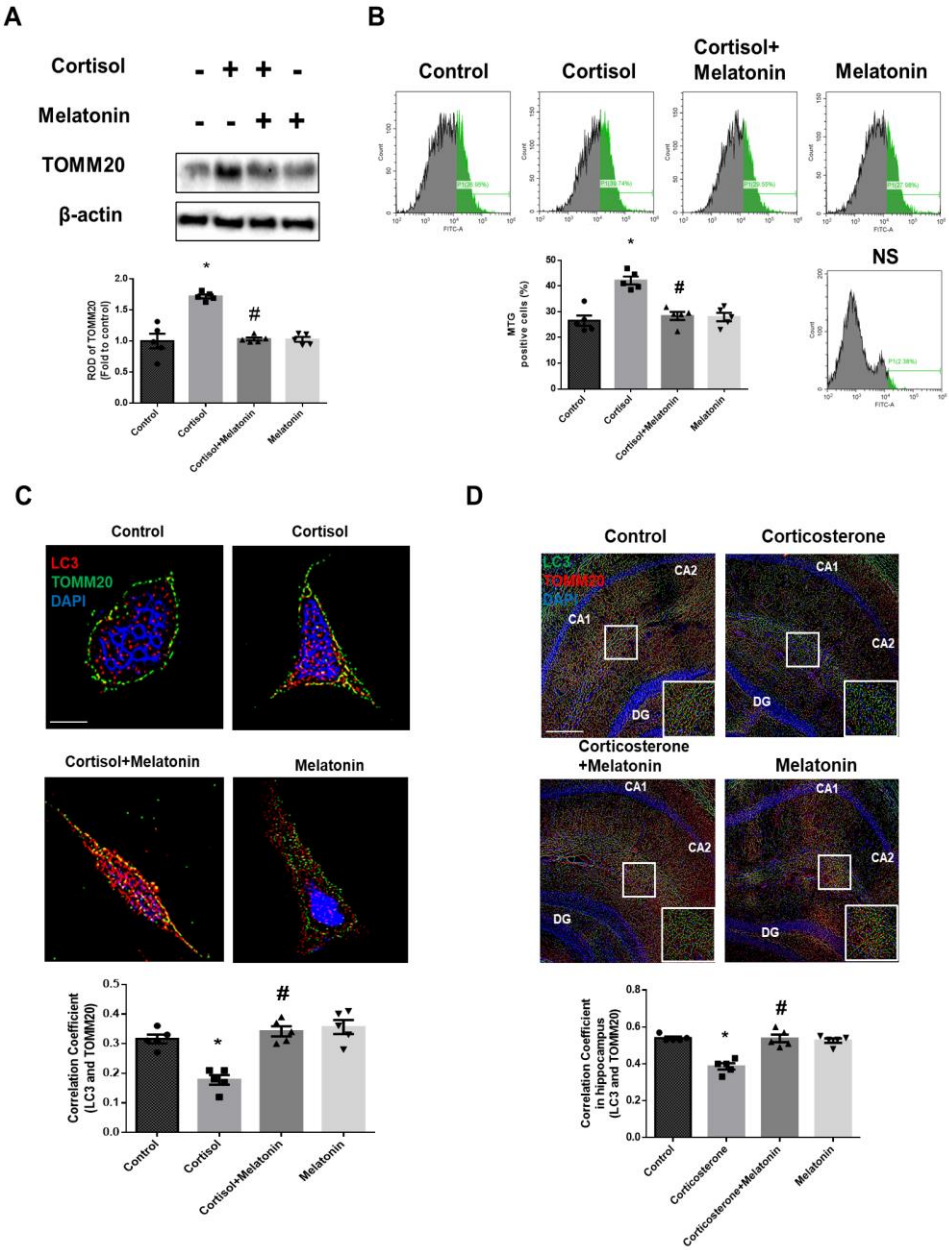
A
Cortisol
Melatonin
TOMM20
β-actin
ROD of TOMM20 (Fold to control)
Control
Cortisol
Cortisol+Melatonin
Melatonin
B
Control
Cortisol
Cortisol+ Melatonin
Melatonin
MTG positive cells (%)
NS
C
Control
Cortisol
LC3
TOMM20
DAPI
Cortisol+Melatonin
Melatonin
Correlation Coefficient (LC3 and TOMM20)
D
Control
Corticosterone
CA1
CA2
DG
Corticosterone +Melatonin
Melatonin
Correlation Coefficient in hippocampus (LC3 and TOMM20)

Figure 1. Effect of melatonin on the glucocorticoid-induced defective mitophagy. SH-SY5Y cells were treated with melatonin (1 μM) for 30 min and then with cortisol (1 μM) for 24 h. (A) Protein levels of TOMM20 were investigated by western blot. Loading control is β-actin. n = 5. (B) After incubation, MTG (200 nM) was stained to detect mitochondrial contents. n = 5. (C) SH-SY5Y cells were immunostained with LC3 (red), TOMM20 (green) and DAPI (blue). Scale bars, 10 μm (magnification, ×1,000). n = 5. (D) Mice were injected with melatonin (10 mg/kg) for 30 min and then with corticosterone (10 mg/kg) for 7 days. Slide samples for IHC were immunostained with LC3 (green), TOMM20 (red), and DAPI (blue). Scale bars, 140 μm (magnification, ×100). n = 5. All blots and immunofluorescence images are representative. All data are presented as a mean ± S.E.M. $*p < 0.05$ versus control, $^{\#}p < 0.05$ versus cortisol or corticosterone. NS means non-staining.

A

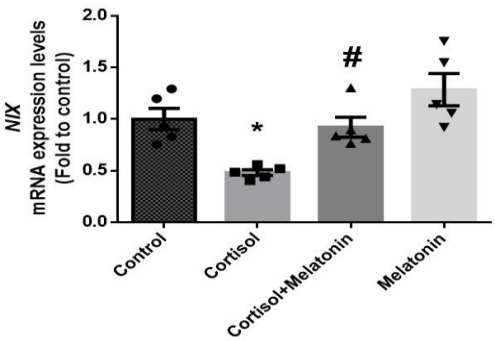
NIX
mRNA expression levels
(Fold to control)
2.0
1.5
1.0
0.5
0.0
*
#
Control
Cortisol
Cortisol+Melatonin
Melatonin

B

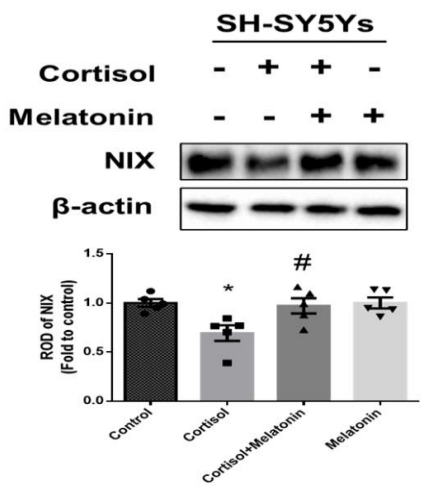
SH-SY5Ys
Cortisol - + + -
Melatonin - - + +
NIX
β-actin
ROD of NIX
(Fold to control)
1.5
1.0
0.5
0.0
*
#
Control
Cortisol
Cortisol+Melatonin
Melatonin

C

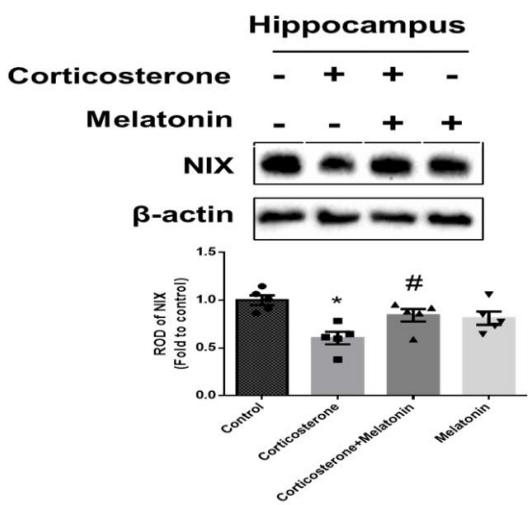
Hippocampus
Corticosterone - + + -
Melatonin - - + +
NIX
β-actin
ROD of NIX
(Fold to control)
1.5
1.0
0.5
0.0
*
#
Control
Corticosterone
Corticosterone+Melatonin
Melatonin

Figure 2. Melatonin improves glucocorticoid-induced NIX-mediated defective mitophagy. (A) Cells were treated with melatonin for 30 min and then with cortisol for 12 h. The mRNA expression of *NIX* was analyzed by real time PCR. $n = 5$. (B) SH-SY5Y cells were treated with melatonin (1 μM) for 30 min and then with cortisol (1 μM) for 24 h. NIX was detected by western blot. Loading control is β-actin. $n = 5$. (C) Mice were injected with melatonin (10 mg/kg) for 30 min and then with corticosterone (10 mg/kg) for 7 days. NIX was detected by western blot. Loading control is β-actin. $n = 5$. All blots and immunofluorescence images are representative. All data are presented as a mean ± S.E.M. $*p < 0.05$ versus control, $^{\#}p < 0.05$ versus cortisol or corticosterone.

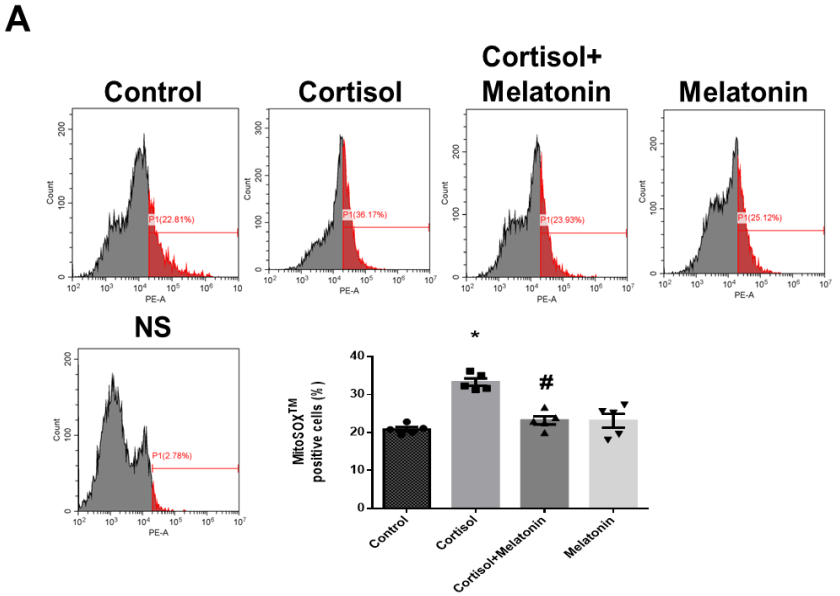
A
Control
Cortisol
Cortisol+ Melatonin
Melatonin
NS
P1(22.81%)
P1(36.17%)
P1(23.93%)
P1(25.12%)
P1(2.78%)
PE-A
Count
MitoSOX™ positive cells (%)
Control
Cortisol
Cortisol+Melatonin
Melatonin

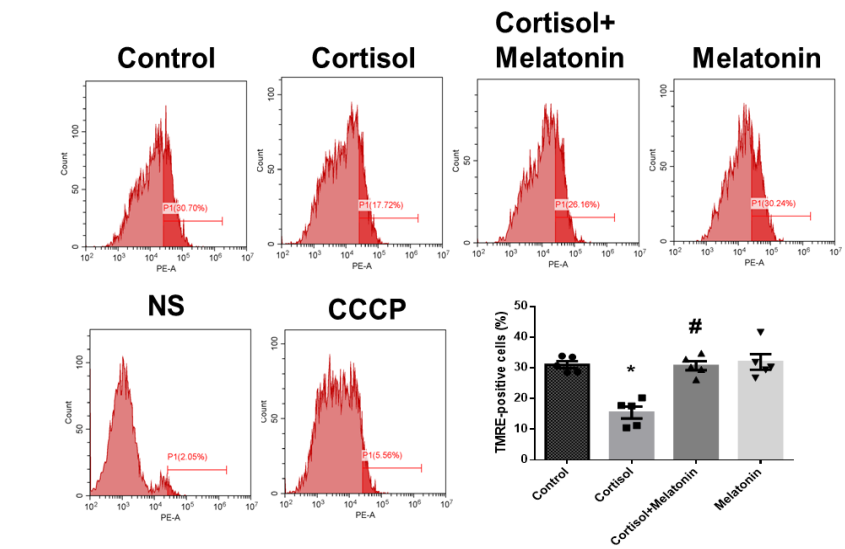
B
Control
Cortisol
Cortisol+ Melatonin
Melatonin
NS
CCCP
P1(30.70%)
P1(17.72%)
P1(28.16%)
P1(30.24%)
P1(2.05%)
P1(5.56%)
PE-A
Count
TMRE-positive cells (%)
Control
Cortisol
Cortisol+Melatonin
Melatonin

Figure 3. Effect of melatonin on the glucocorticoid-induced mitochondrial dysfunction. (A) SH-SY5Y cells were treated with melatonin (1 μM) for 30 min and then with cortisol (1 μM) for 24 h. The population of MitoSOX™ -positive cells were measured by flow cytometry. n = 5. (B) SH-SY5Y cells were treated with melatonin for 30 min and then with cortisol for 48 h. Mitochondrial membrane potential was measured via TMRE staining detected with flow cytometry. n = 5. All data are presented as a mean ± S.E.M. $*p < 0.05$ versus control, $^{\#}p < 0.05$ versus cortisol.

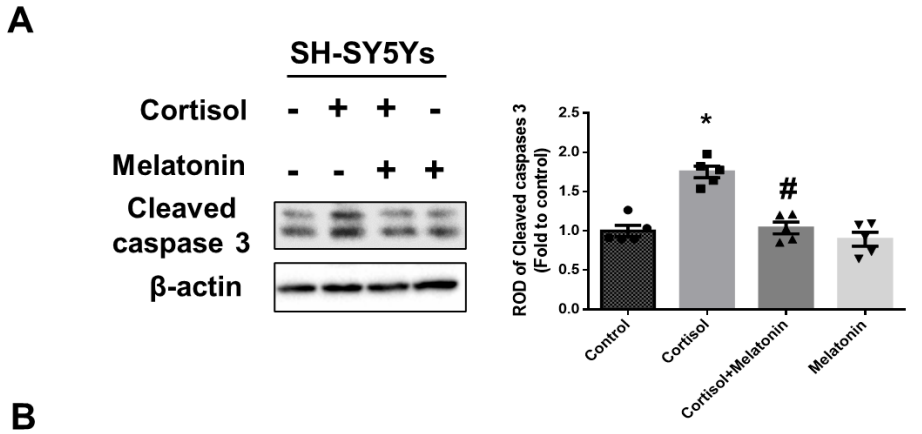
A
SH-SY5Ys
Cortisol - + + -
Melatonin - - + +
Cleaved caspase 3
β-actin
ROD of Cleaved caspases 3 (Fold to control)
Control
Cortisol
Cortisol+Melatonin
Melatonin

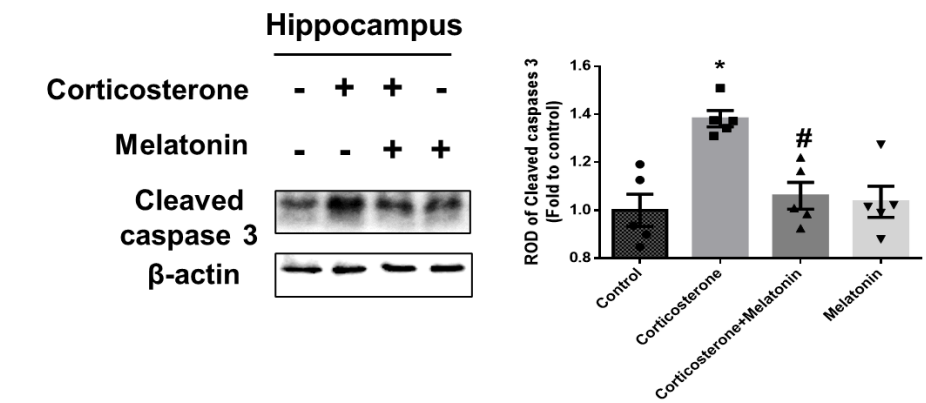
B
Hippocampus
Corticosterone - + + -
Melatonin - - + +
Cleaved caspase 3
β-actin
ROD of Cleaved caspases 3 (Fold to control)
Control
Corticosterone
Corticosterone+Melatonin
Melatonin

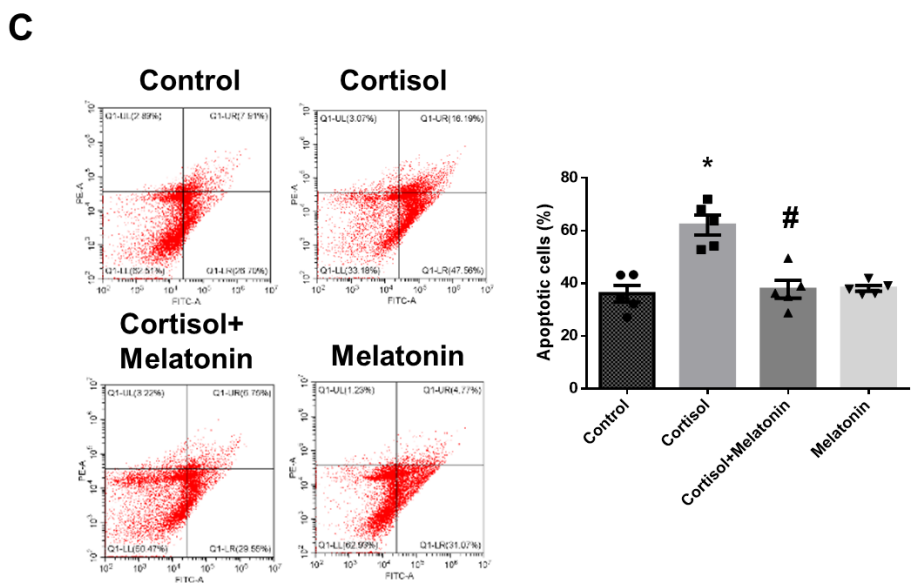
C
Control
Cortisol
Cortisol+ Melatonin
Melatonin
Apoptotic cells (%)
Control
Cortisol
Cortisol+Melatonin
Melatonin

Figure 4. Effect of melatonin on the glucocorticoid-induced neuronal cell death. (A) SH-SY5Y cells were treated with melatonin for 30 min and then with cortisol for 48 h. The expression of cleaved-caspase 3 was detected with western blot. Loading control is β-actin. n = 5. (B) Mice were injected with melatonin (10 mg/kg) for 30 min and then with corticosterone (10 mg/kg) for 7 days. The expression of cleaved-caspase 3 was detected with western blot. Loading control is β-actin. n = 5. (C) SH-SY5Y cells were treated with melatonin for 30 min and treated with melatonin for 72 h. Quantitative analysis of fold changes in apoptotic cells was measured by using annexin V/PI staining with flow cytometry. n = 5. All data are presented as a mean ± S.E.M. $*p < 0.05$ versus control, $^{\#}p < 0.05$ versus cortisol or corticosterone.

A

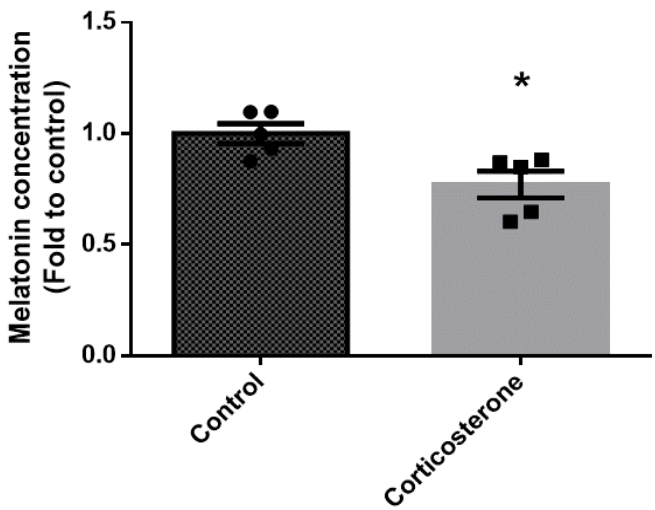
Melatonin concentration
(Fold to control)
1.5
1.0
0.5
0.0
*
Control
Corticosterone

Figure 5. The concentration of melatonin in the plasma of glucocorticoid-exposed mice. (A) Mice were injected with melatonin (10 mg/kg) for 30 min and then with corticosterone (10 mg/kg) for 7 days. Blood was collected from abdominal aorta of mouse groups, and then plasma was isolated. Plasma melatonin level was measured using ELISA. $n = 5$. All data are presented as a mean ± S.E.M. $*p < 0.05$ versus control.

A

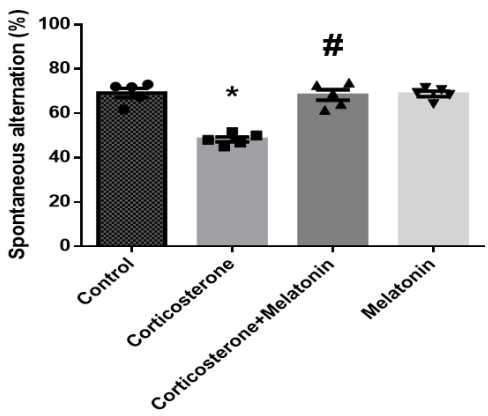
Spontaneous alternation (%)
100
80
60
40
20
0
*
#
Control
Corticosterone
Corticosterone+Melatonin
Melatonin

B

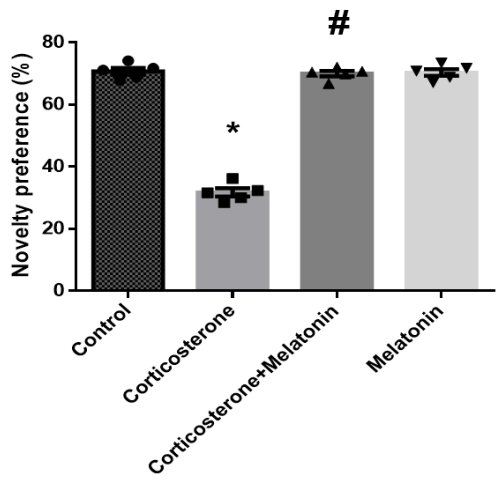
Novelty preference (%)
80
60
40
20
0
*
#
Control
Corticosterone
Corticosterone+Melatonin
Melatonin

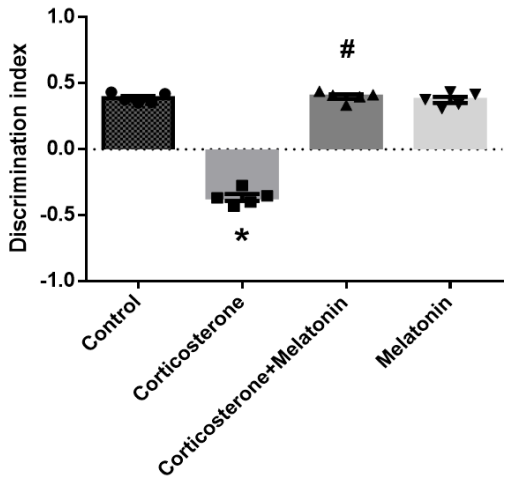
Discrimination index
1.0
0.5
0.0
-0.5
-1.0
*
#
Control
Corticosterone
Corticosterone+Melatonin
Melatonin

Figure 6. Impaired spatial and object working memory was restored by melatonin in glucocorticoid-exposed mice. Mice were injected with melatonin (10 mg/kg) for 30 min and then with corticosterone (10 mg/kg) for 7 days. (A, B) To evaluate spatial and object working memory function, mice were subjected to the Y-maze test and novel object recognition test. $n = 5$. All data are presented as a mean ± S.E.M. $*p < 0.05$ versus control, $^{\#}p < 0.05$ versus corticosterone.

2. Melatonin suppresses glucocorticoid-induced nuclear translocation of GR by down-regulating FKBP4

I assumed that melatonin decreased GR nuclear translocation because glucocorticoid down-regulated NIX expression via the GR-PGC1α-NIX axis (Choi et al., 2021). GR acts as hormone-dependent transcriptional factors regulating the expression of glucocorticoid-responsive genes when translocated into the nucleus (Nicolaides et al., 2020). The phosphorylation of GR on Ser211 increases the level of transcriptional activity because it facilitates nuclear translocation and binding affinity to GR (Galliher-Beckley & Cidlowski, 2009; Wang et al., 2002; Zhang et al., 2009). By western blotting, phosphorylation, the active form of GR and total GR expression were detected. In my data, GR expression did not change, but phosphorylation of GR increased with cortisol. Meanwhile, melatonin did not reduce cortisol-induced phosphorylation of GR, suggesting that melatonin did not participate in post-translational modification of GR (Fig. 7A). These results indicated that melatonin reduced the nuclear import of GR in other mechanisms. My data showed that melatonin reduced the nuclear import of GR in both western blot and immunofluorescence staining

results (Fig. 7B and 7C). In addition, nuclear GR was increased by corticosterone in immunostaining results of the hippocampus, which was reduced by melatonin (Fig. 7D). Therefore, I screened the expression of potential proteins that affect GR nuclear translocation. The proteins that form a complex with GR in the cytoplasm or promote nuclear trafficking and NPC proteins were screened. In my data, melatonin only reduced mRNA expression of *FKBP52*, which is known as a co-chaperone protein that enters the nucleus with the help of dynein and facilitates GR trafficking into the nucleus (Fig. 8A). Consistently, FKBP4 expression detected by western blot was only significantly down-regulated by melatonin treatment in both SH-SY5Y cells and hippocampus (Fig. 8B and 8C). Accordingly, I focused on the role of FKBP4 in GR trafficking and how it changes with melatonin.

Without ligand, GR binds to FKBP5 to retain itself in the cytosolic compartment. Conversely, when the ligand is bound, the co-chaperone protein FKBP4 allows GR to enter the nucleus attaching to dynein. In other words, GR moves into the nucleus in a ligand-dependent manner when binding to FKBP5 is changed into FKBP4. Thus, I further investigated the binding status of FKBP4 or FKBP5 to GR. Compared with the interaction between FKBP5 and GR, the binding of FKBP4 to GR increased following cortisol treatment, which

was reduced by melatonin (Fig. 9A). In PLA and immunostaining results, melatonin treatment reduced the cortisol-induced co-localization between GR and FKBP4 (Fig. 9B and 9C). Collectively, I assumed that melatonin-induced FKBP4 down-regulation would prevent dynein-mediated nuclear translocation of GR. To determine whether reduced FKBP4 affects the dynein-dependent nuclear translocation of GR, the co-localization between GR and dynein was checked. My data showed that GR-dynein interaction was increased by glucocorticoids, which was suppressed by melatonin in both SH-SY5Y cells and hippocampal tissue (Fig. 10A and 10B). Additionally, the interaction of GR with NUP62 and importin β was also checked. My data showed that the interaction of both NUP62 and importin β with GR was increased by glucocorticoids, which were both inhibited by melatonin in SH-SY5Y cells (Fig. 10C and 10D). Taken together, because melatonin inhibits FKBP4 expression, decreased binding between GR and FKBP4 results in suppressed nuclear translocation of GR.

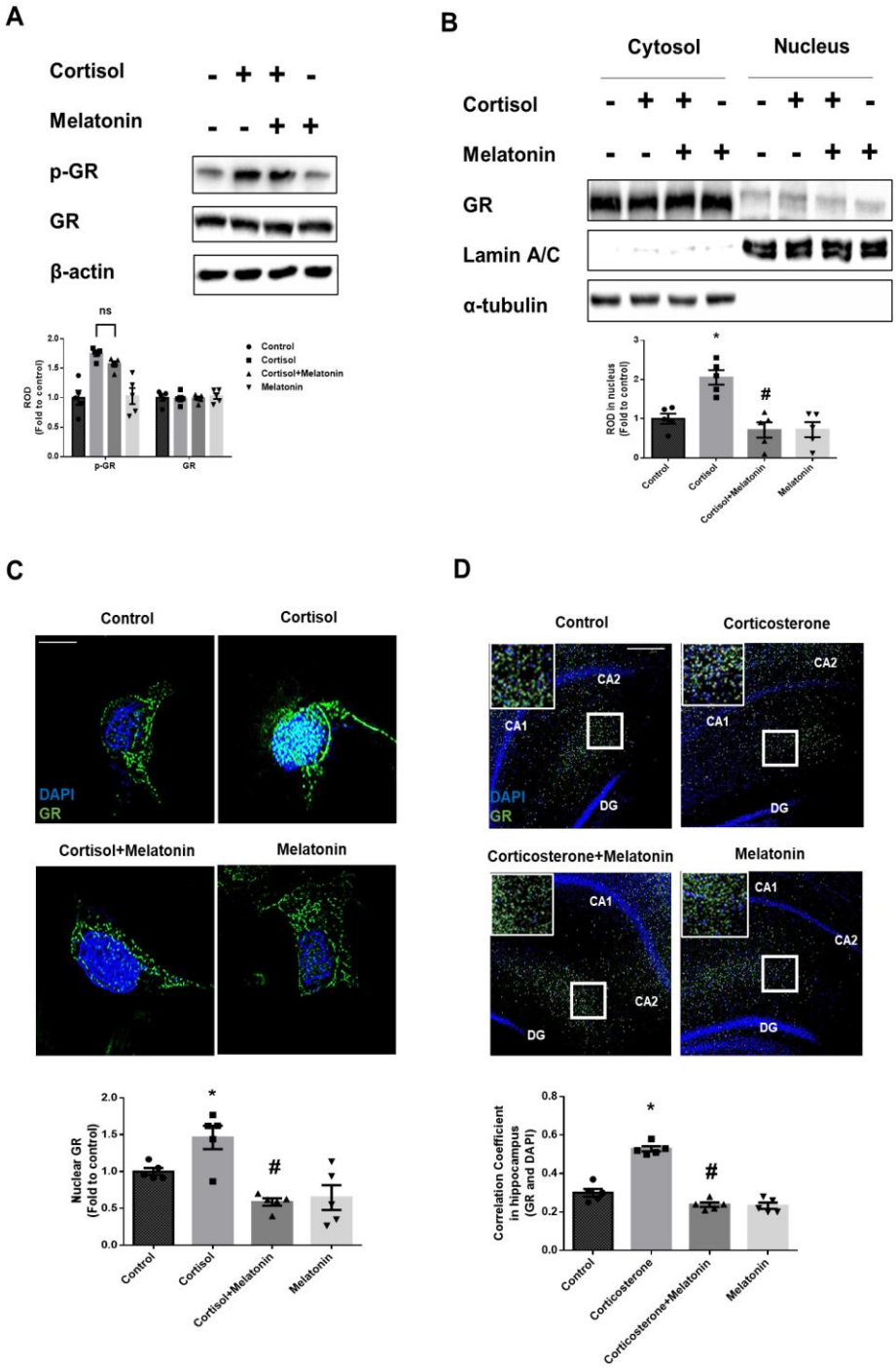
A
Cortisol
Melatonin
p-GR
GR
β-actin
ns
ROD (Fold to control)
p-GR
GR
Control
Cortisol
Cortisol+Melatonin
Melatonin
B
Cytosol
Nucleus
Cortisol
Melatonin
GR
Lamin A/C
α-tubulin
ROD in nucleus (Fold to control)
Control
Cortisol
Cortisol+Melatonin
Melatonin
C
Control
Cortisol
DAPI
GR
Cortisol+Melatonin
Melatonin
Nuclear GR (Fold to control)
Control
Cortisol
Cortisol+Melatonin
Melatonin
D
Control
Corticosterone
CA1
CA2
DG
DAPI
GR
Corticosterone+Melatonin
Melatonin
Correlation Coefficient in hippocampus (GR and DAPI)
Control
Corticosterone
Corticosterone+Melatonin
Melatonin

Figure 7. Melatonin blocks GR nuclear translocation. SH-SY5Y cells were treated with melatonin (1 μM) for 30 min and then with cortisol (1 μM) for 24 h. (A) The expression of p-GR and GR were detected by western blot. Loading control is β-actin. n = 5. (B) The expression of GR protein in subcellular fraction samples was detected by western blotting. Lamin A/C and α-tubulin were used as a nuclear and cytosolic loading control, respectively. n = 5. (C) The cells were immunostained with GR (green) and DAPI (blue). Scale bars, 10 μm (magnification, ×1,000). n = 5. (D) Mice were injected with melatonin (10 mg/kg) for 30 min and then with corticosterone (10 mg/kg) for 7 days. Slide samples for IHC were immunostained with GR (green) and DAPI (blue). Scale bars, 140 μm (magnification, ×100). n = 5. All data are presented as a mean ± S.E.M. $*p < 0.05$ versus control, $^{\#}p < 0.05$ versus cortisol or corticosterone.

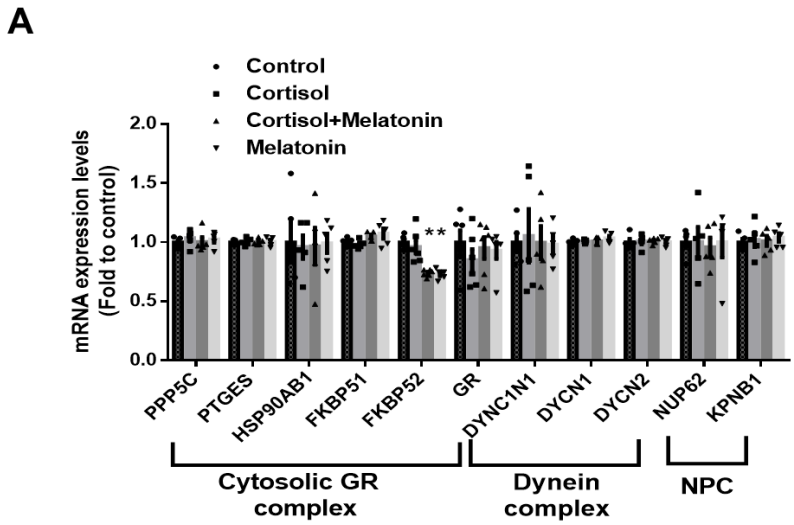
A
Control
Cortisol
Cortisol+Melatonin
Melatonin
mRNA expression levels
(Fold to control)
2.0
1.5
1.0
0.5
0.0
**
PPP5C
PTGES
HSP90AB1
FKBP51
FKBP52
GR
DYNC1N1
DYCN1
DYCN2
NUP62
KPNB1
Cytosolic GR complex
Dynein complex
NPC

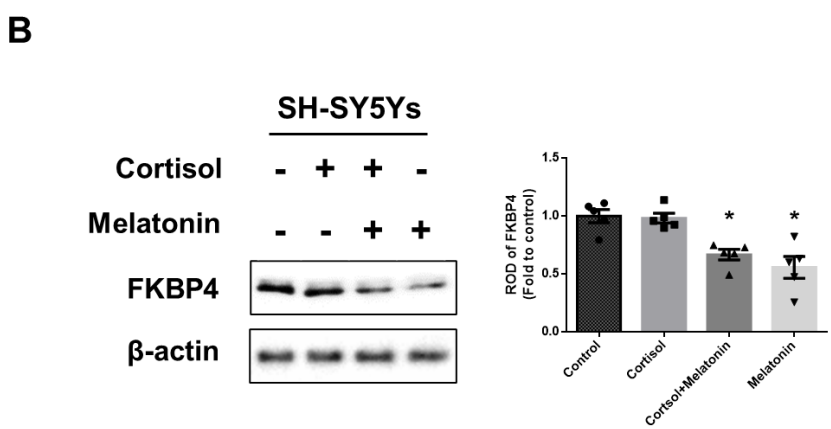
B
SH-SY5Ys
Cortisol - + + -
Melatonin - - + +
FKBP4
β-actin
ROD of FKBP4
(Fold to control)
1.5
1.0
0.5
0.0
*
*
Control
Cortisol
Cortsol+Melatonin
Melatonin

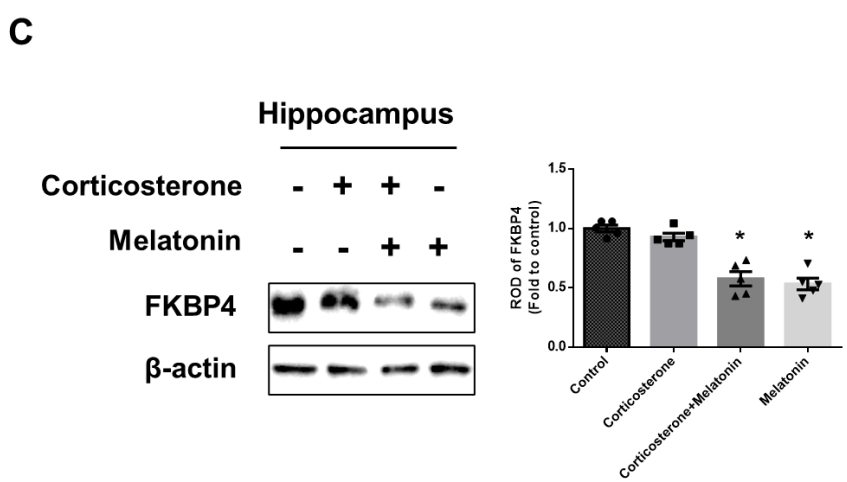
C
Hippocampus
Corticosterone - + + -
Melatonin - - + +
FKBP4
β-actin
ROD of FKBP4
(Fold to control)
1.5
1.0
0.5
0.0
*
*
Control
Corticosterone
Corticosterone+Melatonin
Melatonin

Figure 8. Involvement of FKBP4 in GR nuclear translocation. (A) SH-SY5Y cells were treated with melatonin for 30 min and then with cortisol for 12 h. The mRNA expression of regulatory proteins related to cytosolic GR complex, dynein complex, and NPC were analyzed by real time PCR. n = 5. (B) SH-SY5Y cells were treated with melatonin (1 μM) for 30 min and then with cortisol (1 μM) for 24 h. FKBP4 was detected by western blot. Loading control is β-actin. n = 5. (C) Mice were injected with melatonin (10 mg/kg) for 30 min and then with corticosterone (10 mg/kg) for 7 days. FKBP4 was detected by western blot. Loading control is β-actin. n = 5. All data are presented as a mean ± S.E.M. $^{*}p < 0.05$ versus control, $^{\#}p < 0.05$ versus cortisol or corticosterone.

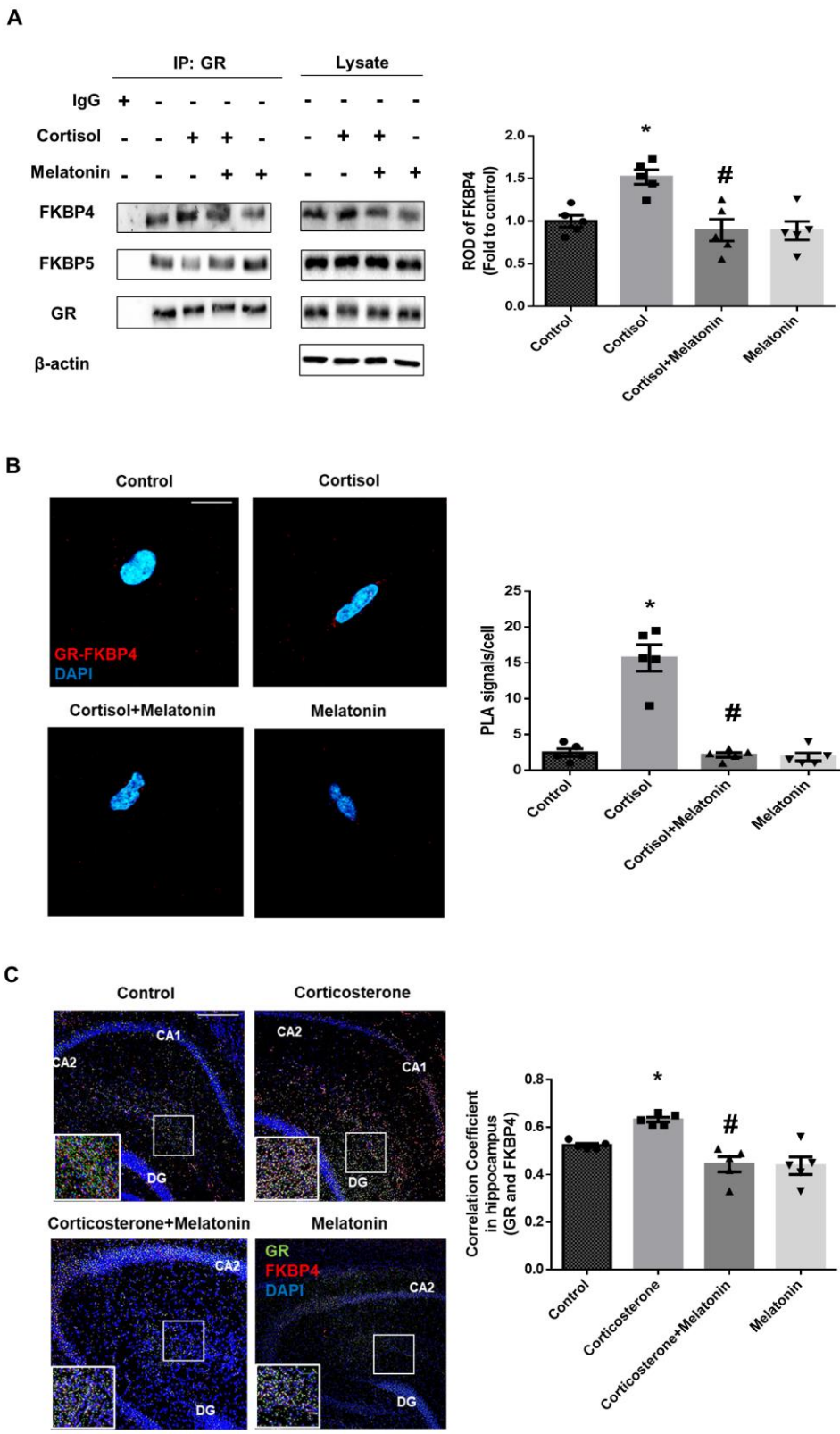
A
IP: GR
Lysate
IgG
Cortisol
Melatonin
FKBP4
FKBP5
GR
β-actin
ROD of FKBP4 (Fold to control)
Control
Cortisol
Cortisol+Melatonin
Melatonin
B
Control
Cortisol
GR-FKBP4
DAPI
Cortisol+Melatonin
Melatonin
PLA signals/cell
C
Control
Corticosterone
CA1
CA2
DG
Corticosterone+Melatonin
Melatonin
GR
FKBP4
DAPI
Correlation Coefficient in hippocampus (GR and FKBP4)

Figure 9. Effect of FKBP4 down-regulation on co-localization between GR and FKBP4. SH-SY5Y cells were treated with melatonin (1 μM) for 30 min and then with cortisol (1 μM) for 24 h. (A) GR was co-immunoprecipitated with FKBP4 and FKBP5. The level of FKBP4 protein in immunoprecipitated samples was quantified. n = 5. (B) The interaction between GR and FKBP4 was investigated via PLA. Scale bars, 10 μm (magnification, ×1,000). n = 5. (C) Mice were injected with melatonin (10 mg/kg) for 30 min and then with corticosterone (10 mg/kg) for 7 days. Slide samples for IHC were immunostained with GR (green), FKBP4 (red) and DAPI (blue). Scale bars, 140 μm (magnification, ×100). n = 5. All data are presented as a mean ± S.E.M. $*p < 0.05$ versus control, $^{\#}p < 0.05$ versus cortisol or corticosterone.

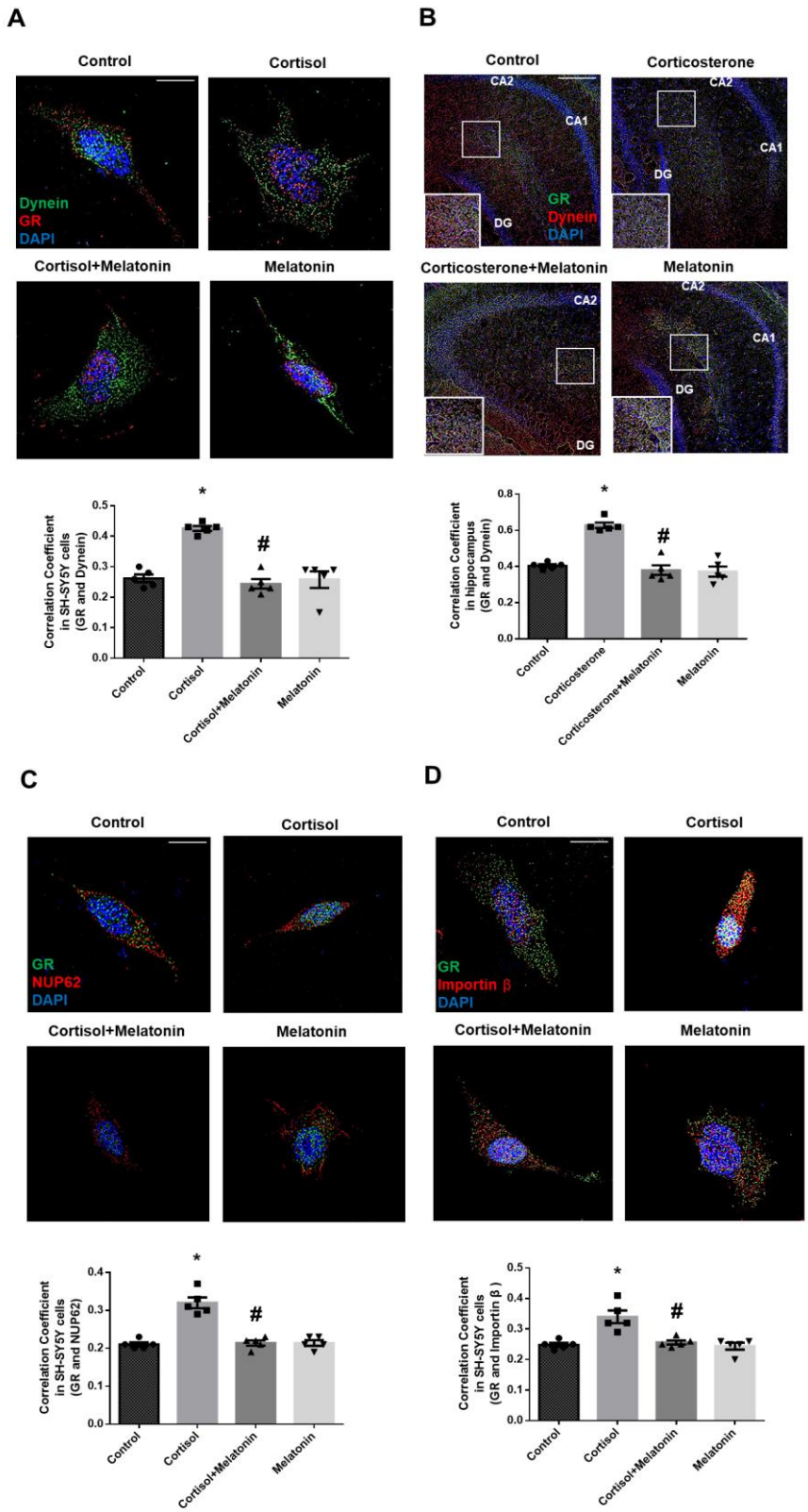
A
Control
Cortisol
Dynein
GR
DAPI
Cortisol+Melatonin
Melatonin
Correlation Coefficient in SH-SY5Y cells (GR and Dynein)
Control
Cortisol
Cortisol+Melatonin
Melatonin
B
Control
Corticosterone
CA2
CA1
DG
GR
Dynein
DAPI
Corticosterone+Melatonin
Melatonin
Correlation Coefficient in hippocampus (GR and Dynein)
Control
Corticosterone
Corticosterone+Melatonin
Melatonin
C
Control
Cortisol
GR
NUP62
DAPI
Cortisol+Melatonin
Melatonin
Correlation Coefficient in SH-SY5Y cells (GR and NUP62)
Control
Cortisol
Cortisol+Melatonin
Melatonin
D
Control
Cortisol
GR
Importin β
DAPI
Cortisol+Melatonin
Melatonin
Correlation Coefficient in SH-SY5Y cells (GR and Importin β)
Control
Cortisol
Cortisol+Melatonin
Melatonin

Figure 10. Effect of FKBP4 down-regulation on co-localization between GR and nuclear trafficking proteins. SH-SY5Y cells were treated with melatonin (1 μM) for 30 min and then with cortisol (1 μM) for 24 h. Mice were injected with melatonin (10 mg/kg) for 30 min and then with corticosterone (10 mg/kg) for 7 days. (A) The cells were immunostained with GR (red), dynein (green) and DAPI (blue). Scale bars, 10 μm (magnification, ×1,000). n = 5. (B) Slide samples for IHC were immunostained with dynein (red), GR (green), and DAPI (blue). Scale bars, 140 μm (magnification, ×100). n = 5. (C) The cells were immunostained with GR (green), NUP62 (red), and DAPI (blue). Scale bars, 10 μm (magnification, ×1,000). n = 5. (D) The cells were immunostained with GR (green), importin β (red), and DAPI (blue). Scale bars, 10 μm (magnification, ×1,000). n = 5. All data are presented as a mean ± S.E.M. $^{*}p < 0.05$ versus control, $^{\#}p < 0.05$ versus cortisol or corticosterone.

3. Melatonin down-regulates FKBP4 by promoting hypermethylation through DNMT1 up-regulation

I investigated by which factors melatonin down-regulates FKBP4 expression. First, to determine whether the expression is regulated by transcription factors, the mRNA level of *FKBP52* was checked by treating actinomycin D, which is known as a transcription factor inhibitor. As shown, melatonin-induced down-regulation in *FKBP52* mRNA expression was maintained in a reduced state even with actinomycin D treatment (Fig. 11A). Therefore, I focused on the epigenetics of down-regulating FKBP4 and screened for relevant epigenetics-related proteins such as histone deacetylase (HDAC) or DNMT. Isoforms of HDAC class I including HDAC 1, 2, 3 and 8 are highly expressed in brain regions (Gibson & Murphy, 2010). In general, there are 3 types of DNMTs in the body; DNMT1, DNMT3a, and DNMT3b. Thus, the expressions of HDAC class I proteins and three major DNMTs were checked by PCR. My data revealed that the reduction of FKBP4 expression may be mainly due to DNMT1 up-regulation (Fig. 11B). In the western blot results, DNMT1 protein level was increased by melatonin, but there was no

change in its expression when exposed to glucocorticoid treatment (Fig. 11C and 11D). Then, I determined which type of melatonin receptor mainly up-regulates DNMT1. In mammals, there are two major melatonin receptors MT1 and MT2. As shown, melatonin increased the expression of *MT1* mRNA, whereas that of *MT2* was unchanged (Fig. 12A). However, cortisol did not change the expression of MT receptors (Fig. 12B). Moreover, western blotting results revealed that melatonin increased the expression levels of MT1 proteins (Fig. 12C). Furthermore, *MT1* knockdown reduced the effects of melatonin on FKBP4 down-regulation. My data showed that FKBP4 was down-regulated by mediating MT1-dependent pathways of melatonin (Fig. 12D). MT receptors belong to the G-protein coupled receptor especially known to bind to Gαq (Jockers et al., 2008; Peschke et al., 2013). Moreover, immunofluorescence confirmed that melatonin increased the interaction between Gαq and MT1 (Fig 13A). The Gαq-mediated pathway activates MAPK by PKC-dependent pathways (Goldsmith & Dhanasekaran, 2007). The mammalian MAPK includes three subfamilies ERK, JNK, and p38. To determine which MAPKs are affected by melatonin, western blotting was performed. My results showed with melatonin treatment, ERK phosphorylation was increased, whereas other MAPK activities were not changed (Fig. 13B). In addition, ERK activation was reduced

through *MT1* knockdown (Fig. 13C). Among the transcription factors phosphorylated by ERK, c-MYC is known to regulate DNMT1, which suggests that melatonin increased c-MYC phosphorylation in an ERK-dependent manner (Xu et al., 2019). In addition, I observed whether ERK activates serine 62 of c-MYC, a transcription factor that regulates DNMT1 expression. My ICC data showed that melatonin increased phosphorylated c-MYC at serine 62 (Fig. 13D). In the western blot result, phosphorylated c-MYC was reduced by pretreatment with the ERK inhibitor PD98059 (Fig. 13E). Furthermore, my data showed that melatonin enhanced the nuclear translocation of c-MYC (Fig. 13F). Altogether, DNMT1, a protein that may inhibit FKBP4 expression, was up-regulated by melatonin through the MT1/ERK/c-MYC pathway.

Then, I investigated whether melatonin-induced DNMT1 up-regulation reduced FKBP4 expression by hypermethylating its promoter. Initially, I checked whether the binding of SP1, known as the transcription factor of *FKBP52,* to its promoter was reduced by melatonin-mediated hypermethylation. In addition, to determine whether FKBP4 down-regulation is dependent on DNMT, the DNMT inhibitor 5-aza was used. The results of my ChIP assay in SH-SY5Y cells showed that the binding of SP1 to *FKBP52* promoter was reduced with melatonin treatment, but was reverted

by 5-aza (Fig. 14A). In general, DNMT1 methylates the CpG site of the promoter, which represses gene expression. Therefore, to evaluate the level of methylation in melatonin-treated groups, a dot blot assay was conducted. This assay was conducted by using 5-mc, which normally occurs at the CpG site where methylation occurs. In this study, melatonin increased the methylation level, which was not changed in the cortisol-treated group (Fig. 14B). Furthermore, MSP was performed to measure the specific methylation status of the *FKBP4* promoter containing CpG sites. Expectedly, methylation occurred near the promoter of *FKBP52* and was increased by melatonin compared with the control group (Fig. 14C). To confirm that DNMT1 had an inhibitory effect on FKBP4 expression, cells were transfected with *DNMT1* siRNA. FKBP4 transcription and protein expression were decreased by melatonin whereas knockdown of *DNMT1* reversed these effects (Fig. 15A and 15B). Overall, melatonin-induced DNMT1 inhibits the expression of FKBP4 by methylating its promoter, thereby repressing gene expression. Then, I examined whether melatonin-mediated DNMT1 down-regulation improves mitochondrial function by promoting mitophagy. My MTG results showed that melatonin reversed cortisol-induced increase in mitochondrial contents, but these effects were abolished by the *DNMT1* knockdown (Fig. 16A).

Furthermore, cortisol-induced reduction of mitochondrial potential was reversed by *DNMT1* knockdown (Fig. 16B). SH-SY5Y cells underwent significant apoptosis when exposed to cortisol but were recovered by melatonin, the effect of which was reduced by *DNMT1* knockdown (Fig. 16C). In summary, glucocorticoid-induced mitophagy impairment and subsequent mitochondrial homeostasis were recovered by melatonin-induced DNMT1 up-regulation.

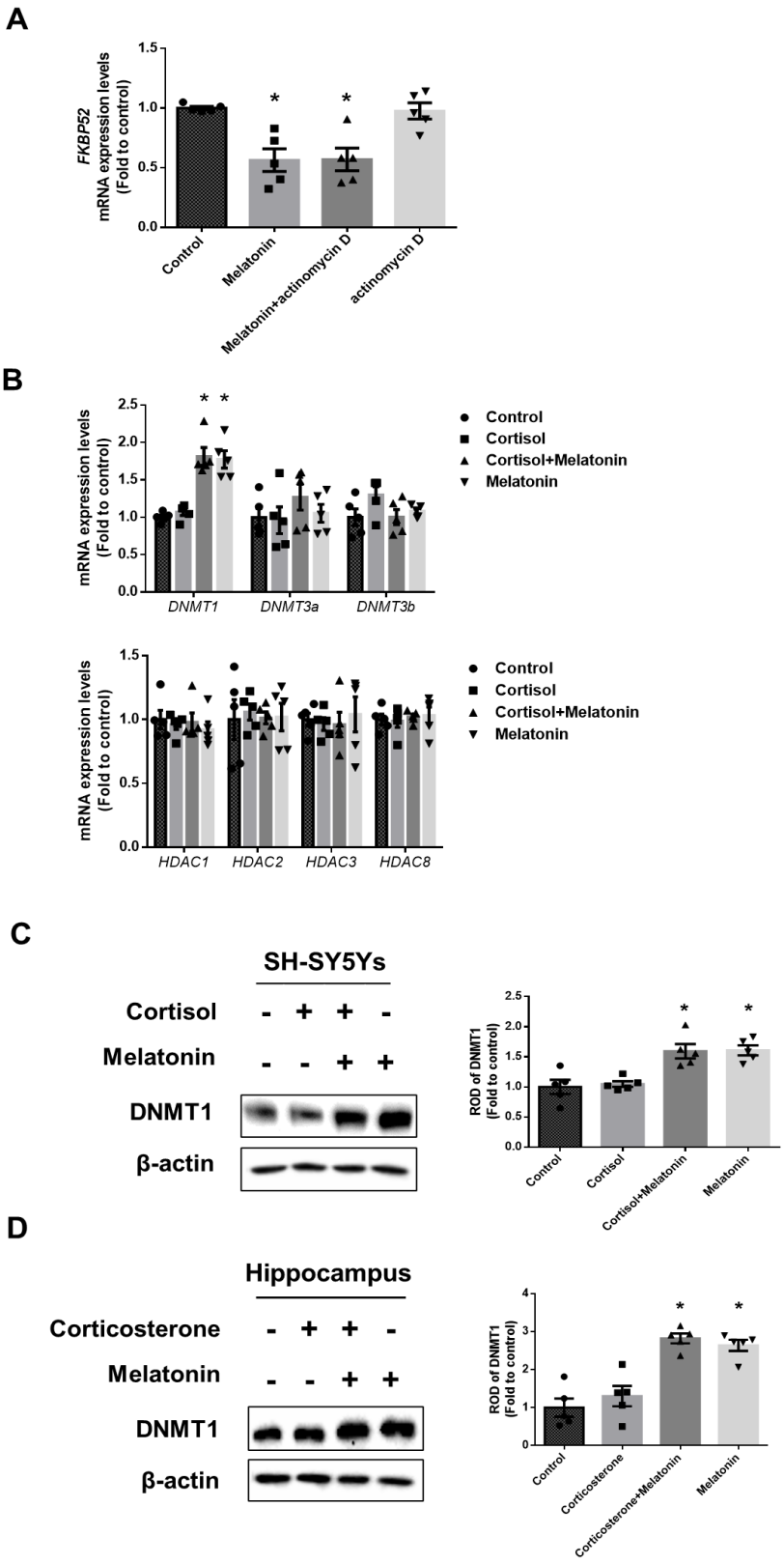
A
FKBP52 mRNA expression levels (Fold to control)
1.5
1.0
0.5
0.0
*
*
Control
Melatonin
Melatonin+actinomycin D
actinomycin D
B
mRNA expression levels (Fold to control)
2.5
2.0
1.5
1.0
0.5
0.0
* *
DNMT1
DNMT3a
DNMT3b
Control
Cortisol
Cortisol+Melatonin
Melatonin
mRNA expression levels (Fold to control)
1.5
1.0
0.5
0.0
HDAC1
HDAC2
HDAC3
HDAC8
Control
Cortisol
Cortisol+Melatonin
Melatonin
C
SH-SY5Ys
Cortisol - + + -
Melatonin - - + +
DNMT1
β-actin
ROD of DNMT1 (Fold to control)
2.5
2.0
1.5
1.0
0.5
0.0
* *
Control
Cortisol
Cortisol+Melatonin
Melatonin
D
Hippocampus
Corticosterone - + + -
Melatonin - - + +
DNMT1
β-actin
ROD of DNMT1 (Fold to control)
4
3
2
1
0
* *
Control
Corticosterone
Corticosterone+Melatonin
Melatonin

Figure 11. Involvement of DNMT1 in the down-regulation of FKBP4. SH-SY5Y cells were treated with melatonin (1 μM) for 30 min and then with cortisol (1 μM) for 12 h. (A) The cells were treated with actinomycin D (500 ng/ml) 30 min before treating melatonin and cortisol. The *FKBP52* mRNA expression was analyzed by real time PCR. n = 5. (B) The mRNA expression of epigenetic-regulated genes was analyzed by real time PCR. n = 5. (C) SH-SY5Y cells were treated with melatonin for 30 min and then with cortisol for 24 h. DNMT1 expression was detected by western blot. Loading control is β-actin. n = 5. (D) Mice were injected with melatonin (10 mg/kg) for 30 min and then with corticosterone (10 mg/kg) for 7 days. DNMT1 expression was detected by western blot. Loading control is β-actin. n = 5. All data are presented as a mean $\pm$ S.E.M. $*p < 0.05$ versus control.

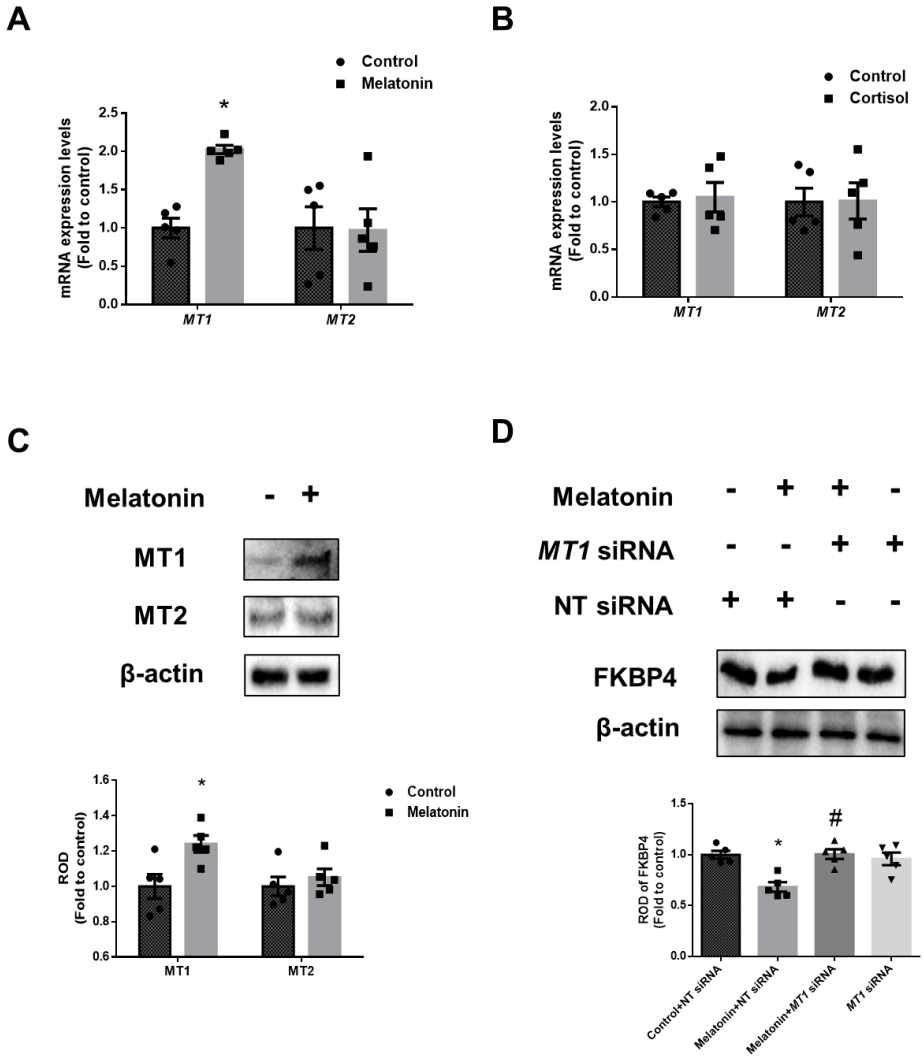
A
Control
Melatonin
mRNA expression levels
(Fold to control)
2.5
2.0
1.5
1.0
0.5
0.0
*
MT1
MT2
B
Control
Cortisol
mRNA expression levels
(Fold to control)
2.0
1.5
1.0
0.5
0.0
MT1
MT2
C
Melatonin - +
MT1
MT2
β-actin
ROD
(Fold to control)
1.6
1.4
1.2
1.0
0.8
0.6
*
MT1
MT2
Control
Melatonin
D
Melatonin - + + -
MT1 siRNA - - + +
NT siRNA + + - -
FKBP4
β-actin
ROD of FKBP4
(Fold to control)
1.5
1.0
0.5
0.0
*
#
Control+NT siRNA
Melatonin+NT siRNA
Melatonin+MT1 siRNA
MT1 siRNA

Figure 12. Involvement of MT1 in down-regulating FKBP4 expression. (A) SH-SY5Y cells were treated with melatonin for 12 h. The *MT1* and *MT2* mRNA expression were analyzed by real time PCR. n = 5. (B) SH-SY5Y cells were treated with cortisol for 12 h. The *MT1* and *MT2* mRNA expression were analyzed by real time PCR. n = 5. (C) MT1 and MT2 levels were detected by western blot. Loading control is β-actin. n = 5. (D) The cells were transfected with NT or *MT1* siRNA 24 h before melatonin treatment for 24 h. FKBP4 levels were detected by western blot. Loading control is β-actin. n = 5. All data are presented as a mean ± S.E.M. $*p < 0.05$ versus control, $^{\#}p < 0.05$ versus melatonin with NT siRNA transfection.

A

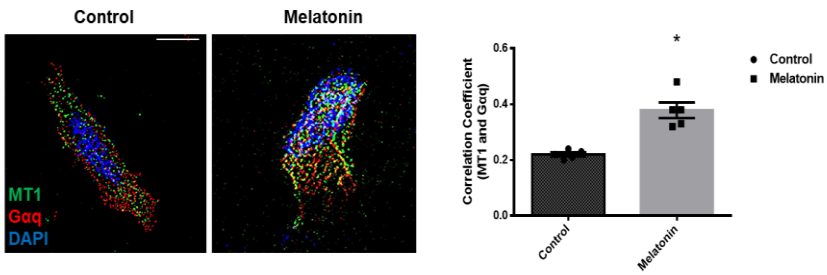
Control
Melatonin
MT1
Gαq
DAPI
Correlation Coefficient (MT1 and Gαq)
0.6
0.4
0.2
0.0
*
Control
Melatonin
Control
Melatonin

B

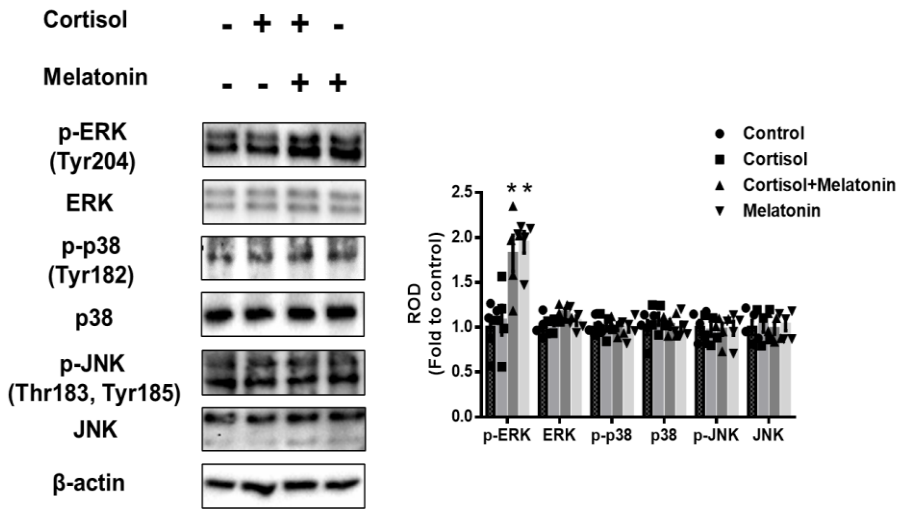
Cortisol - + + -
Melatonin - - + +
p-ERK (Tyr204)
ERK
p-p38 (Tyr182)
p38
p-JNK (Thr183, Tyr185)
JNK
β-actin
Control
Cortisol
Cortisol+Melatonin
Melatonin
ROD (Fold to control)
2.5
2.0
1.5
1.0
0.5
0.0
* *
p-ERK
ERK
p-p38
p38
p-JNK
JNK

C

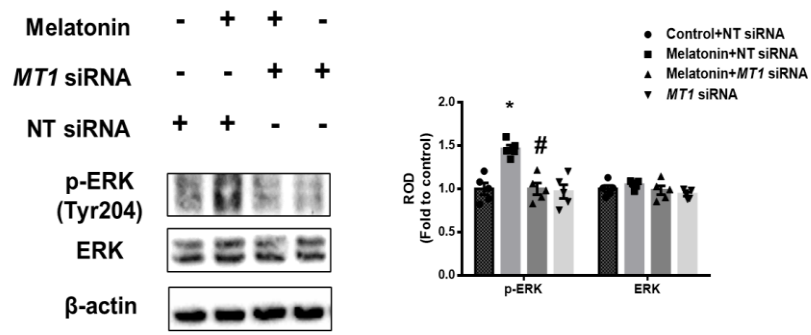
Melatonin - + + -
MT1 siRNA - - + +
NT siRNA + + - -
p-ERK (Tyr204)
ERK
β-actin
Control+NT siRNA
Melatonin+NT siRNA
Melatonin+MT1 siRNA
MT1 siRNA
ROD (Fold to control)
2.0
1.5
1.0
0.5
0.0
*
#
p-ERK
ERK

D

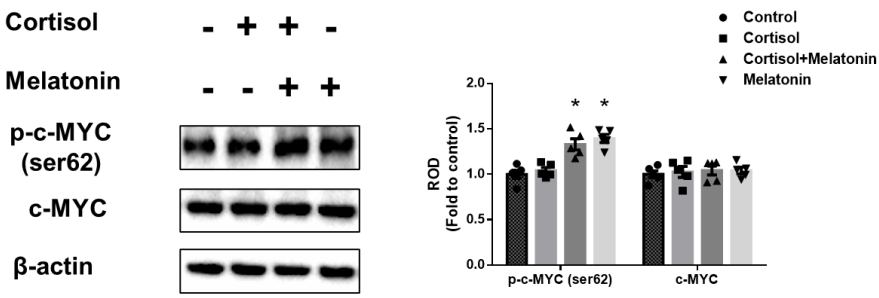
Cortisol
- + + -
Melatonin
- - + +
p-c-MYC (ser62)
c-MYC
β-actin
Control
Cortisol
Cortisol+Melatonin
Melatonin
ROD (Fold to control)
2.0
1.5
1.0
0.5
0.0
* *
p-c-MYC (ser62)
c-MYC

E

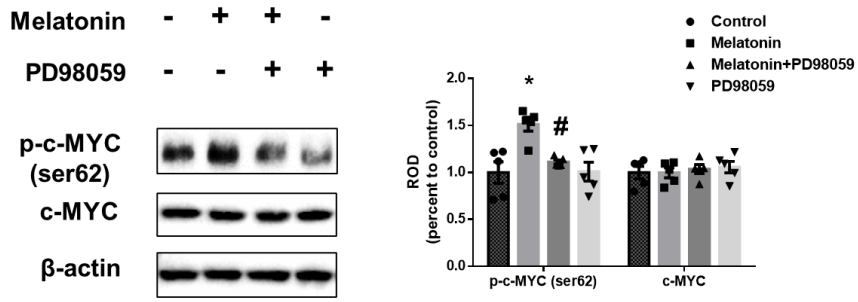
Melatonin
- + + -
PD98059
- - + +
p-c-MYC (ser62)
c-MYC
β-actin
Control
Melatonin
Melatonin+PD98059
PD98059
ROD (percent to control)
2.0
1.5
1.0
0.5
0.0
* #
p-c-MYC (ser62)
c-MYC

F

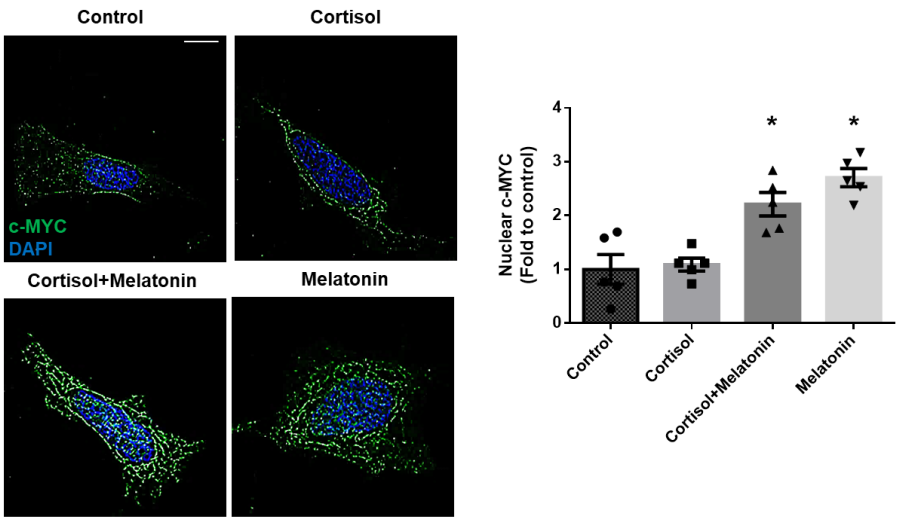
Control
Cortisol
c-MYC
DAPI
Cortisol+Melatonin
Melatonin
Nuclear c-MYC (Fold to control)
4
3
2
1
0
* *
Control
Cortisol
Cortisol+Melatonin
Melatonin

Figure 13. Effect of MT1/ERK/c-MYC signaling on the regulation of DNMT1. SH-SY5Y cells were treated with melatonin (1 μM) for 30 min and then with cortisol (1 μM) for 12 h or SH-SY5Y cells were treated only with melatonin for 12 h. (A) The cells were immunostained with MT1 (green), Gαq (red) and DAPI (blue). Scale bars, 10 μm (magnification, ×1,000). n = 5. (B) The expressions of p-ERK, ERK, p-p38, p38, p-JNK, and JNK were detected by western blot. Loading control is β-actin. n = 5. (C) The cells were transfected with NT or *MT1* siRNA 24 h before melatonin treatment for 12 h. The p-ERK and ERK levels were investigated by western blot. Loading control is β-actin. n = 5. (D) The expressions of p-c-MYC and c-MYC were detected by western blot. Loading control is β-actin. n = 5. (E) PD98059 (50 μM) was treated 30 min before melatonin treatment. The p-c-MYC and c-MYC levels were detected by western blot. Loading control is β-actin. n = 5. (F) The cells were immunostained with c-MYC (green) and DAPI (blue). Scale bars, 10 μm (magnification, ×1,000). n = 5. All data are presented as a mean ± S.E.M. $*p < 0.05$ versus control, $^{\#}p < 0.05$ versus cortisol or corticosterone.

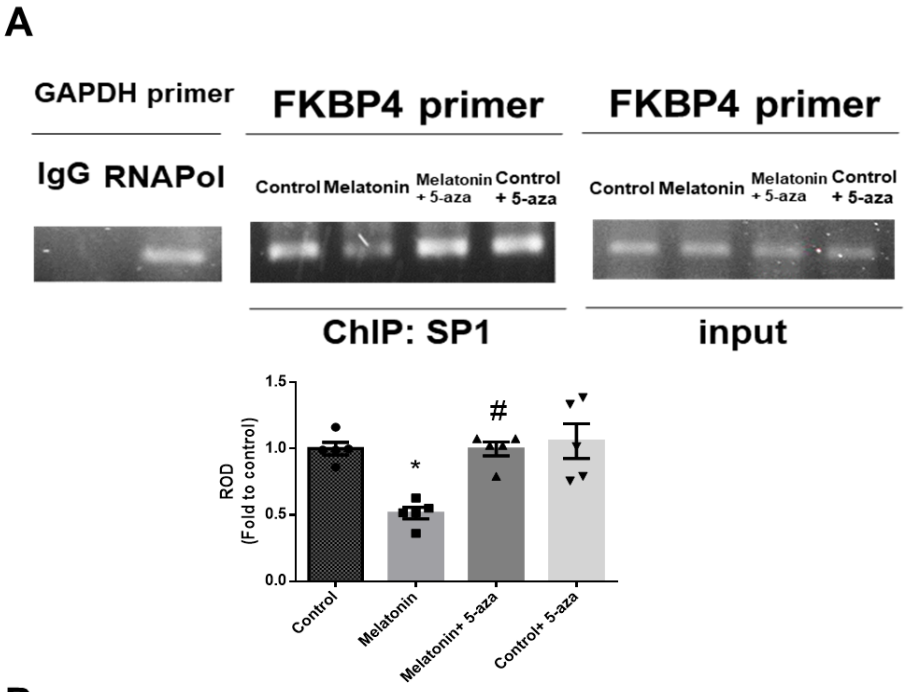
A
GAPDH primer
FKBP4 primer
FKBP4 primer
IgG
RNAPol
Control
Melatonin
Melatonin + 5-aza
Control + 5-aza
Control
Melatonin
Melatonin + 5-aza
Control + 5-aza
ChIP: SP1
input
ROD (Fold to control)
1.5
1.0
0.5
0.0
*
#
Control
Melatonin
Melatonin+ 5-aza
Control+ 5-aza

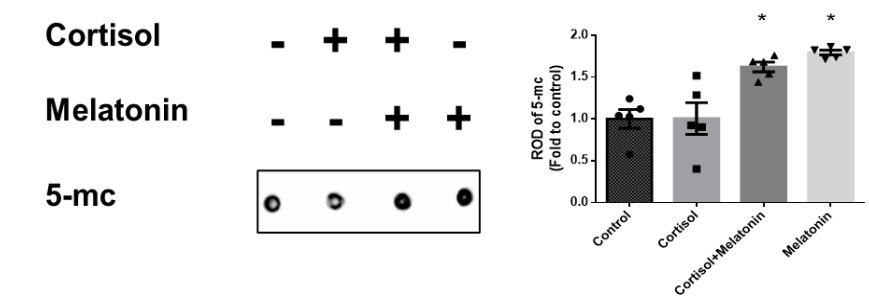
B
Cortisol
Melatonin
5-mc
- + + -
- - + +
ROD of 5-mc (Fold to control)
2.0
1.5
1.0
0.5
0.0
*
*
Control
Cortisol
Cortisol+Melatonin
Melatonin

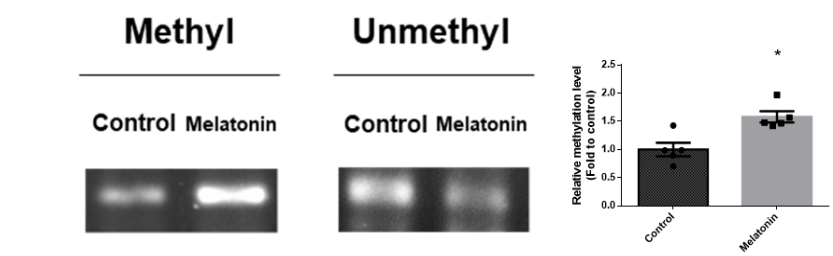
C
Methyl
Unmethyl
Control
Melatonin
Control
Melatonin
Relative methylation level (Fold to control)
2.5
2.0
1.5
1.0
0.5
0.0
*
Control
Melatonin

Figure 14. Effect of melatonin on hypermethylation of FKBP4 promoter. SH-SY5Y cells were treated with melatonin (1 μM) for 30 min and then with cortisol (1 μM) for 12 h. (A) SH-SY5Y cells were treated with 5-aza (10 μM) for 30 min and then treated with melatonin for 12 h. DNA was immunoprecipitated with IgG, RNAPol and SP1 antibody. The immunoprecipitation and input samples were amplified with primers of *GAPDH* and *FKBP52* gene. n = 5. (B) Dot blot assay was performed through DNA extraction. The methylation level was confirmed through 5-mc antibody. n = 5. (C) The methylation status of the CpG region of the *FKBP52* was confirmed in extracted gDNA. n = 5. All data are presented as a mean ± S.E.M. $*p < 0.05$ versus control, $^{\#}p < 0.05$ versus cortisol.

A

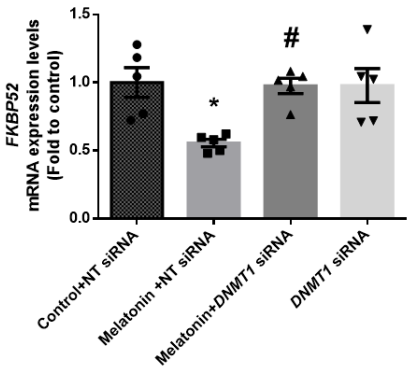
FKBP52
mRNA expression levels
(Fold to control)
1.5
1.0
0.5
0.0
*
#
Control+NT siRNA
Melatonin +NT siRNA
Melatonin+DNMT1 siRNA
DNMT1 siRNA

B

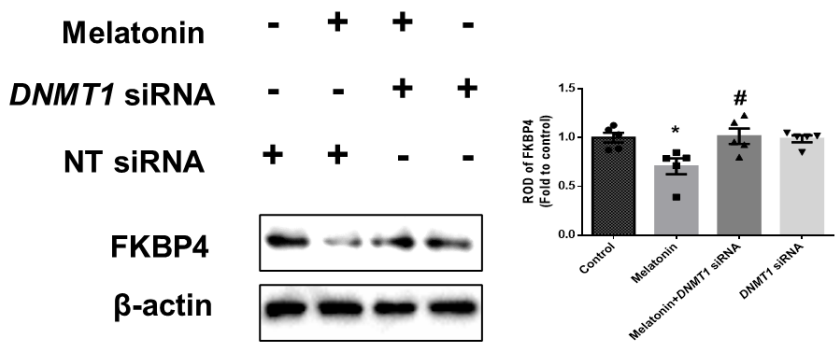
Melatonin - + + -
DNMT1 siRNA - - + +
NT siRNA + + - -
FKBP4
β-actin
ROD of FKBP4
(Fold to control)
1.5
1.0
0.5
0.0
*
#
Control
Melatonin
Melatonin+DNMT1 siRNA
DNMT1 siRNA

Figure 15. DNMT1 down-regulates the expression of FKBP4. (A) The cells were transfected with NT siRNA or *DNMT1* siRNA for 24 h before melatonin treatment for 12 h. The mRNA expression of *FKBP52* were analyzed by quantitative real time PCR. $n = 5$. (B) The cells were transfected with NT siRNA or *DNMT1* siRNA for 24 h before melatonin treatment for 24 h. FKBP4 levels were detected by western blot. Loading control is β-actin. $n = 5$. All data are presented as a mean ± S.E.M. $*p < 0.05$ versus control, $^{\#}p < 0.05$ versus melatonin with *DNMT1* siRNA transfection.

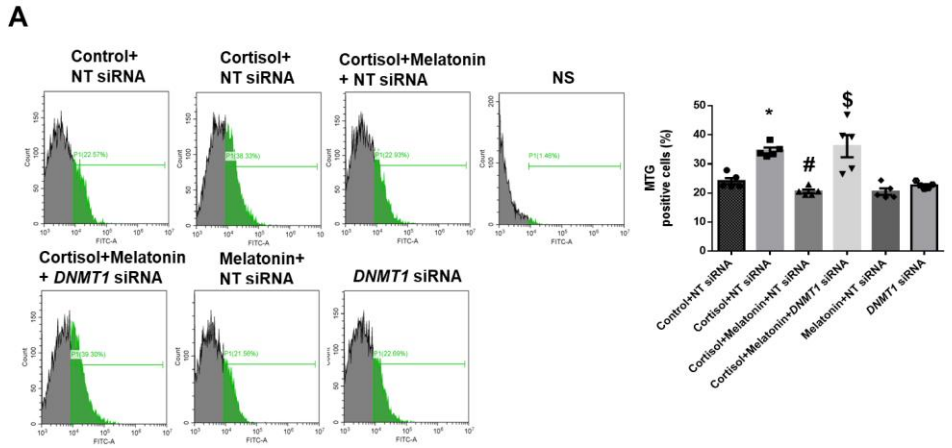
A
Control+
NT siRNA
Cortisol+
NT siRNA
Cortisol+Melatonin
+ NT siRNA
NS
Cortisol+Melatonin
+ DNMT1 siRNA
Melatonin+
NT siRNA
DNMT1 siRNA
MTG
positive cells (%)
Control+NT siRNA
Cortisol+NT siRNA
Cortisol+Melatonin+NT siRNA
Cortisol+Melatonin+DNMT1 siRNA
Melatonin+NT siRNA
DNMT1 siRNA

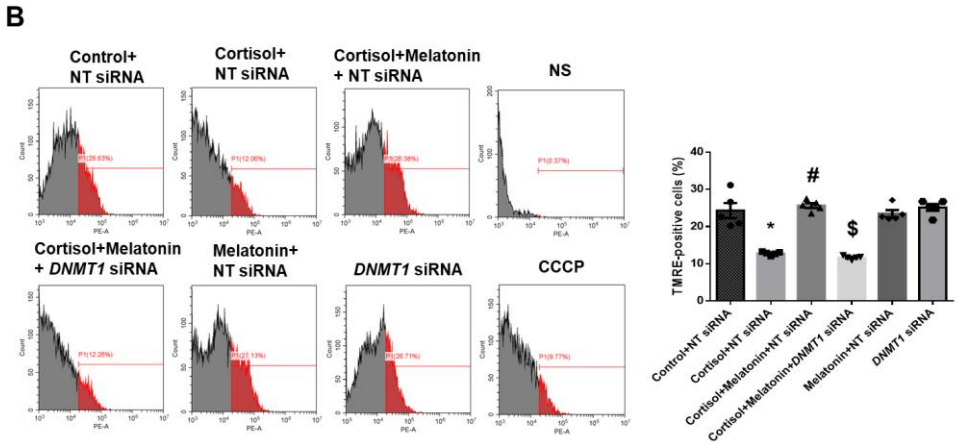
B
Control+
NT siRNA
Cortisol+
NT siRNA
Cortisol+Melatonin
+ NT siRNA
NS
Cortisol+Melatonin
+ DNMT1 siRNA
Melatonin+
NT siRNA
DNMT1 siRNA
CCCP
TMRE-positive cells (%)
Control+NT siRNA
Cortisol+NT siRNA
Cortisol+Melatonin+NT siRNA
Cortisol+Melatonin+DNMT1 siRNA
Melatonin+NT siRNA
DNMT1 siRNA

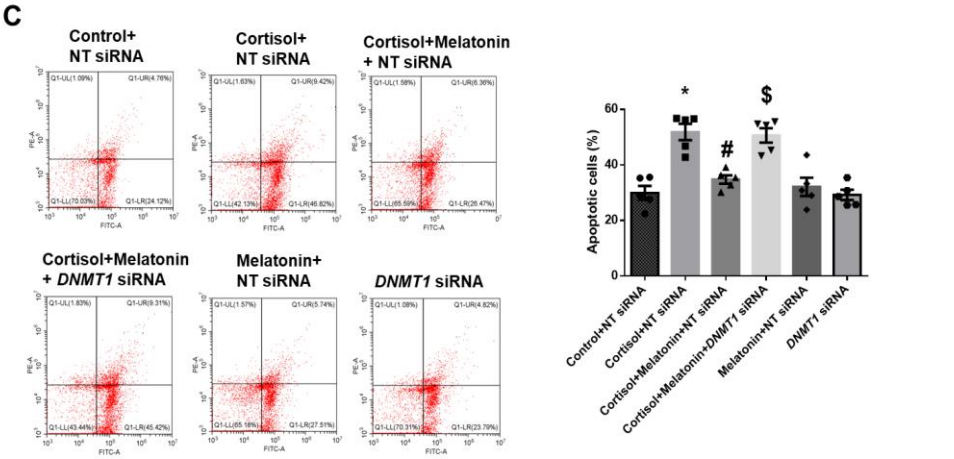
C
Control+
NT siRNA
Cortisol+
NT siRNA
Cortisol+Melatonin
+ NT siRNA
Cortisol+Melatonin
+ DNMT1 siRNA
Melatonin+
NT siRNA
DNMT1 siRNA
Apoptotic cells (%)
Control+NT siRNA
Cortisol+NT siRNA
Cortisol+Melatonin+NT siRNA
Cortisol+Melatonin+DNMT1 siRNA
Melatonin+NT siRNA
DNMT1 siRNA

Figure 16. Effect of DNMT1 on glucocorticoid-induced mitochondrial dysfunction. (A) The cells were transfected with NT siRNA or *DNMT1* siRNA for 24 h before melatonin or cortisol treatment for 24 h. Flow cytometry was used to measure mitochondrial mass by MTG staining. n = 5. (B) The cells were transfected with NT siRNA or *DNMT1* siRNA for 24 h before melatonin or cortisol treatment for 48 h. Flow cytometry was used to detect mitochondrial membrane potential by TMRE staining. n = 5. (C) The cells were transfected with NT siRNA or *DNMT1* siRNA 24 h before melatonin or cortisol treatment for 72 h. Annexin V/PI staining was performed to detect cell apoptosis. n = 5. All data are presented as a mean ± S.E.M. $*p < 0.05$ versus control, $^{\#}p < 0.05$ versus cortisol and $^{\$}p < 0.05$ versus cortisol and melatonin. NS means non-staining.

DISCUSSION

This study provides evidence that melatonin protected both SH-SY5Y cells and hippocampal tissue from glucocorticoid-induced mitochondrial dysfunction and neuronal cell death by blocking GR nuclear translocation through MT1/DNMT1-mediated FKBP4 down-regulation. Melatonin and cortisol are well-known circadian rhythm-related hormones that have opposite functions toward sleep (Fatima et al., 2016). However, when stress activated the hypothalamic-pituitary-adrenal axis (HPA axis), melatonin release is suppressed and its antioxidant mechanism is impaired, resulting in neuronal mitochondrial dysfunction (Karin et al., 2020; Ouanes & Popp, 2019; Zisapel et al., 2005). Consistent with these studies, I revealed that glucocorticoid-induced mitophagy impairment and mitochondrial dysfunction, followed by neuronal cell apoptosis, were well reversed by melatonin treatment in both SH-SY5Y cells and mouse hippocampal tissue. A key function of melatonin is to protect neurons from mitochondrial damage, which protects the brain from neurodegenerative diseases like Alzheimer's disease (AD). For

example, superoxide dismutase is an antioxidant enzyme that is enhanced by melatonin, which inhibits mitochondrial permeability transition pore and promotes mitophagy for clearing dysfunctional mitochondira (Asefy et al., 2021; Cao et al., 2017; Lin et al., 2016; Olakowska et al., 2005). However, suppressing glucocorticoid-induced neurodegenerative pathogenesis by melatonin would be sufficient to restore mitochondrial function and protect neurons from glucocorticoid-mediated neuronal apoptosis. Previous studies have reported that melatonin enhances mitochondrial function by inducing mitophagy, a process of removing damaged mitochondria, and improves cell survival by activating parkin translocation or increasing PINK1 expression (Onphachanh et al., 2017; Wang et al., 2018). However, in my results, melatonin did not solely play an important role in enhancing PINK1-dependent mitophagy or other receptor-mediated mitophagy. Instead, melatonin only recovered NIX expression reduced by excessive glucocorticoids, indicating a possibility that melatonin repressed the GR-PGC1α-NIX axis, as demonstrated by previous study. Melatonin may induce mitophagy-associated regulators except NIX. In fact, several studies have revealed that melatonin enhances mitophagy by the PINK1-parkin pathway or autophagy-related genes in brain ischemia, acute brain injury, or Parkinson's disease models (Lin et al., 2016; Mauri et al.,

2022). However, this study could not detect this phenomenon in hippocampal neurons or SH-SY5Y cells. From these findings, this study can conclude that melatonin has a distinct mechanism to recover NIX-mediated pathways in SH-SY5Y cells and the hippocampus exposed to glucocorticoids. Moreover, melatonin may exert various actions on mitophagy depending on the brain regions or in the presence of high levels of glucocorticoids. Specifically, since the hippocampus is the brain region that has the most GR, it is most affected by glucocorticoids where melatonin-mediated mitophagy and cell survival protection against glucocorticoid action can be more developed in this region. However, whether melatonin simply blocks glucocorticoid action toward mitophagy or whether it has an independent mechanism down-regulating NIX from glucocorticoids need further investigation.

Based on previous study, blocking the activity of GR is important to restore NIX-dependent mitophagy under stress because ligand-bound GR binds to the PGC1α promoter and down-regulates its expression to suppress NIX in neuronal cells (Choi et al., 2021). Through the results, melatonin-mediated suppression on nuclear transport of GRs can solely improve NIX-mediated mitophagy disrupted by glucocorticoids, thereby enhancing mitochondria function and inhibiting neuronal cell death. Several previous studies

have demonstrated the neuroprotective effects of melatonin against glucocorticoid toxicity by blocking GR activity (Aoyama et al., 1987). For example, melatonin directly reduced mRNA expression of corticosteroid receptors in the paraventricular nucleus to counteract glucocorticoid-induced dysregulation of the HPA axis (Konakchieva et al., 1998). However, my results showed no changes in GR expression in neuronal cells. In other studies, melatonin suppressed GR nuclear translocation in thymocytes and peripheral blood mononuclear cells by blocking HSP90 activity (Presman et al., 2006; Quiros et al., 2008; Singh & Haldar, 2016). From these previous findings, the suppressive effect of melatonin in GR action is tissue-specific. However, the exact mechanism of melatonin on suppressing GR nuclear translocation after cytoplasmic retention of GR by HSP90 is not well explored. Therefore, I screened which factor changed upon melatonin mainly participates in suppressing GR nuclear translocation. Under stress, excessive levels of glucocorticoids bound to GRs, which then facilitates dissociation from heat shock proteins. Then, GRs are phosphorylated by several kinases such as MAPKs and CDKs induced by glucocorticoid, and its form can easily move into the nucleus more than GRs by increasing its binding affinity into the glucocorticoid-responsive element of the DNA (Chen et al., 2008;

Galliher-Beckley & Cidlowski, 2009). In this study, as melatonin did not reduce cortisol-induced GR phosphorylation, melatonin is not associated with kinase deactivation toward GR. Instead, melatonin reduced the nuclear transport of GR. With help from association or dissociation with several chaperone proteins, ligand-bound GR is then easily transported into the nucleus. After screening for the related molecules, I found that melatonin blocks the mechanism by which GR-bound chaperone protein is converted from FKBP5 to FKBP4, which makes GR enter the nucleus (Kirschke et al., 2014; Pratt et al., 2006). Interestingly, my data show that among proteins involved in nuclear translocation, FKBP4 expression was only selectively down-regulated by melatonin, which was not changed by glucocorticoid treatment. As GR phosphorylation then contributes to FKBP4-GR binding and subsequent GR nuclear translocation, this study can conclude that GR phosphorylated by cortisol could not sufficiently bind to FKBP4 for nuclear translocation because of melatonin-induced FKBP4 down-regulation (Galigniana et al., 2001; H. Li et al., 2020). FKBP4-GR complex formation is moved into the nucleus with the help of dynein and NPC. Dynein anchors the FKBP4-GR complex into the microtubule and facilitates its passage into the nucleus under NPC supervision. A previous study reported that among other nuclear

pore glycoproteins (NUPs) present in NPC, only NUP62 and importin β affect GR nuclear translocation in human HEK293T cells (Lin et al., 2009; Mazaira et al., 2020). According to my results, melatonin reverted the increased co-localization of dynein/NUPs with GR by glucocorticoid. However, melatonin did not change the mRNA expressions of these genes. Melatonin can have a suppressive effect on this co-localization caused by a reduction in the GR-FKBP4 complex. As the reducing effect of melatonin on nuclear translocation of several transcription factors such as Nrf2 are not related to up-regulating/down-regulating dynein or NUP expression, this study assumed that melatonin mainly participates in regulating chaperone proteins of GR to inhibit its nuclear translocation (Kleszczyński et al., 2016; Premratanachai et al., 2020). Thus, the FKBP4/5 expression ratio can be one of the key regulatory factors for the nuclear retention of steroid receptors. Taken together, the inhibitory effects of melatonin on GR nuclear translocation mainly occurs by down-regulating the FKBP4 complex but not interfering with GR phosphorylation. Therefore, I focused on the down-regulating effects of melatonin on FKBP4 to suppress glucocorticoid-induced neurodegeneration.

When adjusted with transcription inhibitor actinomycin D, melatonin-induced FKBP4 down-regulation was not reversed,

which means that melatonin down-regulated *FKBP4* mRNA expression by regulating epigenetics (Korkmaz & Reiter, 2008). A previous study suggested that melatonin triggered epigenetic regulation in human diseases including neurodegenerative diseases, which indeed affected DNA methylation by regulating DNMT expression (Hardeland, 2019). In agreement with this study, my results also showed that melatonin changed DNMT expression, but it did not trigger a significant change in HDAC expressions. In addition, cortisol can regulate DNMTs in both non-neuronal and neuronal cells (Kantake et al., 2014; Yang et al., 2012). However, my results showed that cortisol is not associated with the expressions of epigenetic-related genes. This can be due to the exposure stage of glucocorticoid;, i.e., glucocorticoid tends to permanently induce epigenetic changes during neurogenesis at the early- or juvenile-stages of mouse models, whereas glucocorticoid-induced changes during adults are usually reversible, regulating transcription with GR (Zhang et al., 2018). Then, this study asked why melatonin selectively increased DNMT1 expression. In human dental pulp cells (hDPCs), melatonin significantly increased DNMT1, but it did not regulate the expressions of DNMT3a and DNMT3b (J. Li et al., 2020; Nie et al., 2018). Consistently, my results showed that DNMT1 is a potent

mediator of melatonin-induced FKBP4 down-regulation in SH-SY5Y cells. Then, I investigated the specific mechanism of how melatonin up-regulated DNMT1 expression. In the mammalian brain, melatonin down-regulates MT2 receptors during peak secretion, while up-regulating MT1. However, the accurate mechanism for MT1 requires further study (Gobbi & Comai, 2019). My data partially agree with this finding in that melatonin increased the expression of MT1, but not the expression of MT2. *MT1* silencing reversed the down-regulating effect of melatonin on FKBP4, suggesting that melatonin increases DNMT1 expression in an MT1 receptor-dependent pathway. Cortisol treatment was not involved in MT expression, indicating that excessive cortisol release in the brain does not enhance melatonin-dependent neuroprotective mechanisms, triggering neurodegeneration. A study reported that dexamethasone modulates melatonin-induced MT2 receptor expression by triggering an immune response in splenic tissue (Singh et al., 2017). These findings indicate that glucocorticoid reduce the melatonin release or MTs to block the action of melatonin. Thus, melatonin-induced boosting of MT receptor activity can protect neurons from GR-mediated neurodegeneration. Based on these results, this study insisted that DNMT1 is regulated in an MT1-dependent manner; then, this study

further investigated the accurate pathway of regulating DNMT1. Given the interaction between Gαq and MT1, which then activates PKC and acts as a critical component of the circadian effect of melatonin, this study screened the downstream signals of PKC (Ahn et al., 2004; Pandi-Perumal et al., 2008). Based on a previous report that PKC activates MAPKs, I investigated which MAPK was activated in SH-SY5Y cells (Toyoda et al., 2004). A previous study reported that melatonin activates the MT1/ERK pathway for Schwann cell dedifferentiation and proliferation and enhances osteoblastic differentiation of MC3T3-E1 cells by activating the ERK pathway (Chan et al., 2022; Tiong et al., 2020). Consistent with the results of these previous studies, my data showed that MT1-induced PKC phosphorylates ERK among MAPKs and activates p-ERK, which phosphorylates serine 62 to increase DNMT1 expression (Xu et al., 2019). This study can then conclude that DNMT1 up-regulation by melatonin-induced MT1 activation is an important target to reduce glucocorticoid-induced GR trafficking into the nucleus to down-regulate FKBP4. Despite melatonin supplementation, mitochondrial dysfunction and neuronal cell apoptosis were not recovered when DNMT1 was down-regulated, suggesting that mitochondria function is regulated by DNMT1. Therefore, I insist that *DNMT1* knockdown does not reduce FKBP4

expression, leading to mitochondria dysfunction. Taken together, FKBP4 down-regulation through DNMT1-mediated hypermethylation by melatonin prevents GR from translocating into the nucleus.

In conclusion, melatonin-downregulated DNMT1/FKBP4/GR pathway suppressed NIX-dependent mitophagy impairment and subsequent glucocorticoid-induced neuronal cell apoptosis (Fig. 17). This study also suggests the FKBPs as therapeutic targets for the various stress-related neurodegenerative disease.

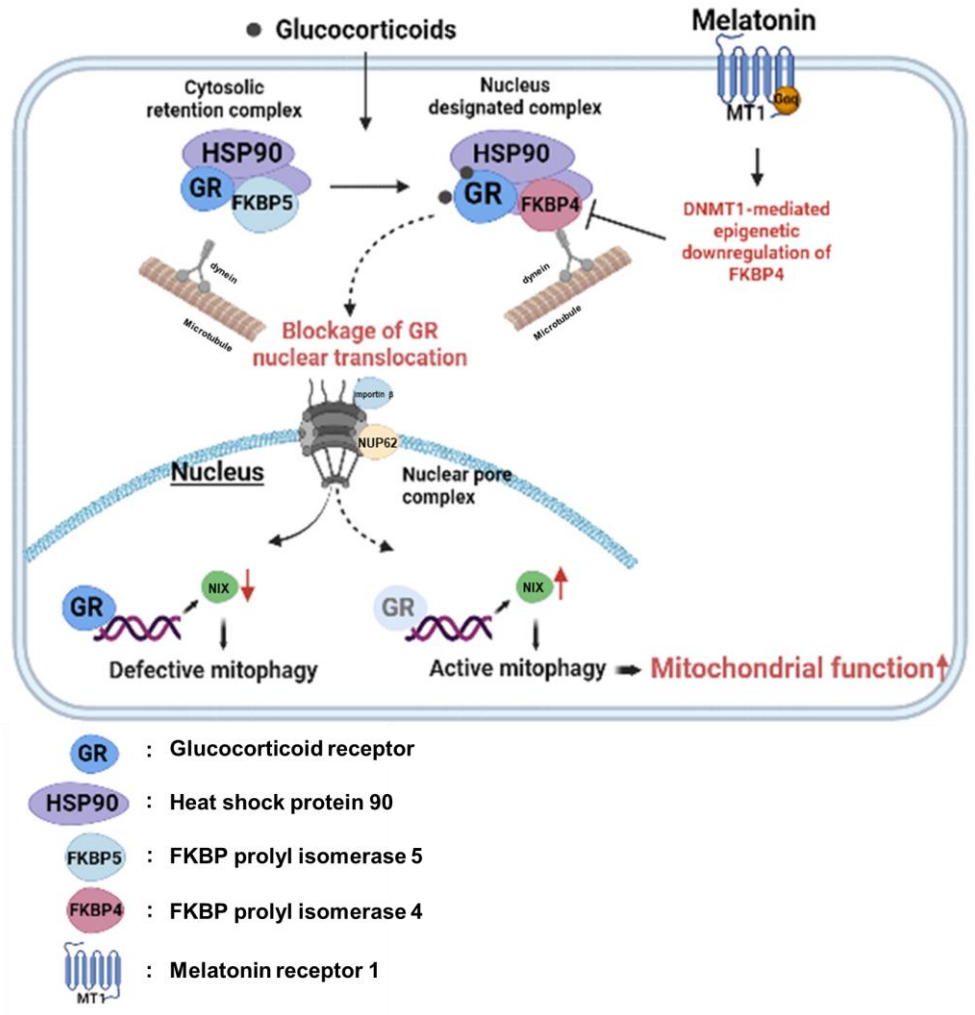

Figure 17. A hypothetical model for improvement of glucocorticoid-induced mitochondrial dysfunction through blocking GR nuclear translocation by melatonin. Glucocorticoid induces nuclear translocation of GR and then represses NIX transcription. Melatonin down-regulates FKBP4 expression by increasing DNMT1 levels to suppress nuclear translocation of GR, which then restores NIX-mediated mitophagy and neuronal cell survival.

REFERENCES

Ahn, S., Wei, H., Garrison, T. R., & Lefkowitz, R. J. (2004). Reciprocal regulation of angiotensin receptor-activated extracellular signal-regulated kinases by β-arrestins 1 and 2. Journal of Biological Chemistry, 279(9), 7807-7811.

Aoyama, H., Mori, N., & Mori, W. (1987). Anti-glucocorticoid effects of melatonin on adult rats. Pathology International, 37(6), 1143-1148.

Asefy, Z., Khusro, A., Mammadova, S., Hoseinnejhad, S., Eftekhari, A., Alghamdi, S., Dablool, A. S., Almehmadi, M., Kazemi, E., & Sahibzada, M. U. K. (2021). Melatonin hormone as a therapeutic weapon against neurodegenerative diseases. Cellular and Molecular Biology, 67(3), 99-106.

Aziz, M. H., Shen, H., & Maki, C. G. (2012). Glucocorticoid receptor activation inhibits p53-induced apoptosis of MCF10Amyc cells via induction of protein kinase Cϵ. Journal of Biological Chemistry, 287(35), 29825-29836.

Bob, P., & Fedor-Freybergh, P. (2008). Melatonin, consciousness, and traumatic stress. Journal of Pineal Research, 44(4), 341-347.

Boga, J. A., Caballero, B., Potes, Y., Perez-Martinez, Z., Reiter, R. J., Vega-Naredo, I., & Coto-Montes, A. (2019). Therapeutic potential of melatonin related to its role as an autophagy regulator: A review. Journal of Pineal Research, 66(1), e12534.

Cao, S., Shrestha, S., Li, J., Yu, X., Chen, J., Yan, F., Ying, G., Gu, C., Wang, L., & Chen, G. (2017). Melatonin-mediated mitophagy protects against early brain injury after subarachnoid hemorrhage through inhibition of NLRP3 inflammasome activation. Scientific Reports, 7(1), 1-11.

Cattaneo, A., & Riva, M. (2016). Stress-induced mechanisms in mental illness: a role for glucocorticoid signalling. The Journal of Steroid Biochemistry and Molecular Biology, 160, 169-174.

Chan, Y.-H., Ho, K.-N., Lee, Y.-C., Chou, M.-J., Lew, W.-Z., Huang, H.-M., Lai, P.-C., & Feng, S.-W. (2022). Melatonin enhances osteogenic differentiation of dental pulp mesenchymal stem cells by regulating MAPK pathways and promotes the efficiency of bone regeneration in calvarial bone defects. Stem Cell Research & Therapy, 13(1), 1-18.

Chen, C., Nakagawa, S., An, Y., Ito, K., Kitaichi, Y., & Kusumi, I. (2017). The exercise-glucocorticoid paradox: How exercise is beneficial to cognition, mood, and the brain while increasing glucocorticoid levels. Frontiers in Neuroendocrinology, 44, 83-102.

Chen, W., Dang, T., Blind, R. D., Wang, Z., Cavasotto, C. N., Hittelman, A. B., Rogatsky, I., Logan, S. K., & Garabedian, M. J. (2008). Glucocorticoid receptor phosphorylation differentially affects target gene expression. Molecular Endocrinology, 22(8), 1754-1766.

Choi, G. E., & Han, H. J. (2021). Glucocorticoid impairs mitochondrial quality control in neurons. Neurobiology of Disease, 152, 105301.

Choi, G. E., Lee, H. J., Chae, C. W., Cho, J. H., Jung, Y. H., Kim, J. S., Kim, S. Y., Lim, J. R., & Han, H. J. (2021). BNIP3L/NIX-mediated mitophagy protects against glucocorticoid-induced synapse defects. Nature Communications, 12(1), 1-18.

Chojnacki, C., Walecka-Kapica, E., Klupinska, G., Pawlowicz, M., Blonska, A., & Chojnacki, J. (2015). Effects of fluoxetine and melatonin on mood, sleep quality and body mass index in postmenopausal women. Journal of Physiology and Pharmacology, 66(5), 665-671.

Clarisse, D., Offner, F., & De Bosscher, K. (2020). Latest perspectives on glucocorticoid-induced apoptosis and resistance in lymphoid malignancies. Biochimica et Biophysica Acta (BBA)-Reviews on Cancer, 1874(2), 188430.

Couto-Moraes, R., Palermo-Neto, J., & Markus, R. P. (2009). The immune-pineal axis: stress as a modulator of pineal gland function. Annals of the New York Academy of Sciences, 1153(1), 193-202.

Da Silveira Cruz-Machado, S., Tamura, E. K., Carvalho-Sousa, C. E., Rocha, V. A., Pinato, L., Fernandes, P. A., & Markus, R. P. (2017). Daily corticosterone rhythm modulates pineal function through NFκB-related gene transcriptional program. Scientific Reports, 7(1), 1-11.

Dagnino-Subiabre, A., Orellana, J. A., Carmona-Fontaine, C., Montiel, J., Díaz-Velíz, G., Serón-Ferré, M., Wyneken, U., Concha, M. L., & Aboitiz, F. (2006). Chronic stress decreases the expression of sympathetic markers in the pineal gland and increases plasma melatonin concentration in rats. Journal of Neurochemistry, 97(5), 1279-1287.

Echeverría, P. C., Mazaira, G., Erlejman, A., Gomez-Sanchez, C., Pilipuk, G. P., & Galigniana, M. D. (2009). Nuclear import of the glucocorticoid receptor-Hsp90 complex through the nuclear pore complex is mediated by its interaction with Nup62 and importin β. Molecular and Cellular Biology, 29(17), 4788-4797.

Fatima, G., Sharma, V., & Verma, N. (2016). Circadian variations in melatonin and cortisol in patients with cervical spinal cord injury. Spinal Cord, 54(5), 364-367.

Galigniana, M. D., Radanyi, C., Renoir, J.-M., Housley, P. R., & Pratt, W. B. (2001). Evidence that the peptidylprolyl isomerase domain of the hsp90-binding immunophilin FKBP52 is involved in both dynein interaction and glucocorticoid receptor movement to the nucleus. Journal of Biological Chemistry, 276(18), 14884-14889.

Galliher-Beckley, A. J., & Cidlowski, J. A. (2009). Emerging roles of glucocorticoid receptor phosphorylation in modulating glucocorticoid hormone action in health and disease. IUBMB Life, 61(10), 979–986.

Gibson, C. L., & Murphy, S. P. (2010). Benefits of histone deacetylase inhibitors for acute brain injury: a systematic review of animal studies. Journal of Neurochemistry, 115(4), 806–813.

Gobbi, G., & Comai, S. (2019). Differential function of melatonin MT1 and MT2 receptors in REM and NREM sleep. Frontiers in Endocrinology, 10, 87.

Goldsmith, Z., & Dhanasekaran, D. (2007). G protein regulation of MAPK networks. Oncogene, 26(22), 3122–3142.

Hardeland, R. (2019). Melatonin and chromatin. Melatonin Research, 2(1), 67–93.

Hoijman, E., Rocha Viegas, L., Keller Sarmiento, M. I., Rosenstein, R. E., & Pecci, A. (2004). Involvement of Bax protein in the prevention of glucocorticoid–induced thymocytes apoptosis by melatonin. Endocrinology, 145(1), 418–425.

Jockers, R., Maurice, P., Boutin, J., & Delagrange, P. (2008). Melatonin receptors, heterodimerization, signal transduction and binding sites: what's new? British Journal of Pharmacology, 154(6), 1182–1195.

Kantake, M., Yoshitake, H., Ishikawa, H., Araki, Y., & Shimizu, T. (2014). Postnatal epigenetic modification of glucocorticoid receptor gene in preterm infants: a prospective cohort study. BMJ open, 4(7), e005318.

Karin, O., Raz, M., Tendler, A., Bar, A., Korem Kohanim, Y., Milo, T., & Alon, U. (2020). A new model for the HPA axis explains dysregulation of stress hormones on the timescale of weeks. Molecular Systems Biology, 16(7), e9510.

Kaziales, A., Barkovits, K., Marcus, K., & Richter, K. (2020). Glucocorticoid receptor complexes form cooperatively with the Hsp90 co-chaperones PP5 and FKBPs. Scientific Reports, 10(1), 1-16.

Kirby, E. D., Muroy, S. E., Sun, W. G., Covarrubias, D., Leong, M. J., Barchas, L. A., & Kaufer, D. (2013). Acute stress enhances adult rat hippocampal neurogenesis and activation of newborn neurons via secreted astrocytic FGF2. Elife, 2, e00362.

Kirschke, E., Goswami, D., Southworth, D., Griffin, P. R., & Agard, D. A. (2014). Glucocorticoid receptor function regulated by coordinated action of the Hsp90 and Hsp70 chaperone cycles. Cell, 157(7), 1685-1697.

Kleszczyński, K., Zillikens, D., & Fischer, T. W. (2016). Melatonin enhances mitochondrial ATP synthesis, reduces reactive oxygen species formation, and mediates translocation of the nuclear erythroid 2-related factor 2 resulting in activation of phase-2 antioxidant enzymes (γ-GCS, HO-1, NQO 1) in ultraviolet radiation-treated normal human epidermal keratinocytes (NHEK). Journal of Pineal Research, 61(2), 187-197.

Konakchieva, R., Mitev, Y., Almeida, O. F., & Patchev, V. K. (1998). Chronic melatonin treatment counteracts glucocorticoid-induced dysregulation of the hypothalamic-pituitary-adrenal axis in the rat. Neuroendocrinology, 67(3), 171-180.

Korkmaz, A., & Reiter, R. J. (2008). Epigenetic regulation: a new research area for melatonin? Journal of Pineal Research, 44(1), 41-44.

Kruk, J., Aboul-Enein, B. H., & Duchnik, E. (2021). Exercise-induced oxidative stress and melatonin supplementation: current evidence. The Journal of Physiological Sciences, 71(1), 1-19.

Li, H., Su, P., Lai, T. K., Jiang, A., Liu, J., Zhai, D., Campbell, C. T., Lee, F. H., Yong, W., & Pasricha, S. (2020). The glucocorticoid receptor–FKBP51 complex contributes to fear conditioning and posttraumatic stress disorder. The Journal of Clinical Investigation, 130(2), 877–889.

Li, J., Deng, Q., Fan, W., Zeng, Q., He, H., & Huang, F. (2020). Melatonin–induced suppression of DNA methylation promotes odontogenic differentiation in human dental pulp cells. Bioengineered, 11(1), 829–840.

Lin, C., Chao, H., Li, Z., Xu, X., Liu, Y., Hou, L., Liu, N., & Ji, J. (2016). Melatonin attenuates traumatic brain injury-induced inflammation: a possible role for mitophagy. Journal of Pineal Research, 61(2), 177–186.

Lin, W., Ye, W., Cai, L., Meng, X., Ke, G., Huang, C., Peng, Z., Yu, Y., Golden, J. A., & Tartakoff, A. M. (2009). The roles of multiple importins for nuclear import of murine aristaless–related homeobox protein. Journal of Biological Chemistry, 284(30), 20428–20439.

Luo, F., Sandhu, A. F., Rungratanawanich, W., Williams, G. E., Akbar, M., Zhou, S., Song, B.–J., & Wang, X. (2020). Melatonin and autophagy in aging–related neurodegenerative diseases. International Journal of Molecular Sciences, 21(19), 7174.

Mauri, S., Favaro, M., Bernardo, G., Mazzotta, G. M., & Ziviani, E. (2022). Mitochondrial autophagy in the sleeping brain. Frontiers in Cell and Developmental Biology, 10, 956394.

Mazaira, G. I., Echeverria, P. C., & Galigniana, M. D. (2020). Nucleocytoplasmic shuttling of the glucocorticoid receptor is influenced by tetratricopeptide repeat–containing proteins. Journal of Cell Science, 133(12), jcs238873.

McWilliams, T. G., Prescott, A. R., Montava-Garriga, L., Ball, G., Singh, F., Barini, E., Muqit, M. M., Brooks, S. P., & Ganley, I.G. (2018). Basal mitophagy occurs independently of PINK1in mouse tissues of high metabolic demand. Cell Metabolism, 27(2), 439-449. e435.

Nicolaides, N. C., Chrousos, G., & Kino, T. (2020). Glucocorticoid receptor. *Endotext*.

Nie, J., Xiao, P., Wang, X., Yang, X., Xu, H., Lu, K., Lu, S., & Liang, X. (2018). Melatonin prevents deterioration in quality by preserving epigenetic modifications of porcine oocytes after prolonged culture. Aging (Albany NY), 10(12), 3897.

Olakowska, E., Marcol, W., Kotulska, K., & Lewin-Kowalik, J. (2005). The role of melatonin in the neurodegenerative diseases. Bratislavske Lekarske Listy, 106(4-5), 171-174.

Onphachanh, X., Lee, H. J., Lim, J. R., Jung, Y. H., Kim, J. S., Chae, C. W., Lee, S. J., Gabr, A. A., & Han, H. J. (2017). Enhancement of high glucose-induced PINK1 expression by melatonin stimulates neuronal cell survival: Involvement of MT2/Akt/NF-κB pathway. Journal of Pineal Research, 63(2), e12427.

Ouanes, S., & Popp, J. (2019). High cortisol and the risk of dementia and Alzheimer's disease: a review of the literature. Frontiers in Aging Neuroscience, 11, 43.

Pandi-Perumal, S. R., Trakht, I., Srinivasan, V., Spence, D. W., Maestroni, G. J., Zisapel, N., & Cardinali, D. P. (2008). Physiological effects of melatonin: role of melatonin receptors and signal transduction pathways. Progress in Neurobiology, 85(3), 335-353.

Peschke, E., Bähr, I., & Mühlbauer, E. (2013). Melatonin and pancreatic islets: interrelationships between melatonin, insulin and glucagon. International Journal of Molecular Sciences, 14(4), 6981-7015.

Pratt, W., Morishima, Y., Murphy, M., & Harrell, M. (2006). Chaperoning of glucocorticoid receptors. Molecular chaperones in Health and Disease, 111-138.

Premratanachai, A., Suwanjang, W., Govitrapong, P., Chetsawang, J., & Chetsawang, B. (2020). Melatonin prevents calcineurin-activated the nuclear translocation of nuclear factor of activated T-cells in human neuroblastoma SH-SY5Y cells undergoing hydrogen peroxide-induced cell death. Journal of Chemical Neuroanatomy, 106, 101793.

Presman, D. M., Hoijman, E., Ceballos, N. R., Galigniana, M. D., & Pecci, A. (2006). Melatonin inhibits glucocorticoid receptor nuclear translocation in mouse thymocytes. Endocrinology, 147(11), 5452-5459.

Quiros, I., Mayo, J. C., Garcia-Suarez, O., Hevia, D., Martin, V., Rodríguez, C., & Sainz, R. M. (2008). Melatonin prevents glucocorticoid inhibition of cell proliferation and toxicity in hippocampal cells by reducing glucocorticoid receptor nuclear translocation. The Journal of Steroid Biochemistry and Molecular Biology, 110(1-2), 116-124.

Scheschowitsch, K., Leite, J., & Assreuy, J. (2017). New insights in glucocorticoid receptor signaling - more than just a ligand binding receptor. Frontiers in Endocrinology, 8.

Schmidt, S., Rainer, J., Ploner, C., Presul, E., Riml, S., & Kofler, R. (2004). Glucocorticoid-induced apoptosis and glucocorticoid resistance: molecular mechanisms and clinical relevance. Cell Death & Differentiation, 11(1), S45-S55.

Singh, A. K., & Haldar, C. (2016). Melatonin modulates glucocorticoid receptor mediated inhibition of antioxidant response and apoptosis in peripheral blood mononuclear cells. Molecular and Cellular Endocrinology, 436, 59-67.

Singh, S. S., Deb, A., & Sutradhar, S. (2017). Dexamethasone modulates melatonin MT2 receptor expression in splenic tissue and humoral immune response in mice. Biological Rhythm Research, 48(3), 425-435.

Tiong, Y. L., Ng, K. Y., Koh, R. Y., Ponnudurai, G., & Chye, S. M. (2020). Melatonin promotes Schwann cell dedifferentiation and proliferation through the Ras/Raf/ERK and MAPK pathways, and glial cell-derived neurotrophic factor expression. Experimental and Therapeutic Medicine, 20(5), 1-1.

Toyoda, M., Suzuki, D., Honma, M., Uehara, G., Sakai, T., Umezono, T., & Sakai, H. (2004). High expression of PKC-MAPK pathway mRNAs correlates with glomerular lesions in human diabetic nephropathy. Kidney International, 66(3), 1107-1114.

Vandevyver, S., Dejager, L., & Libert, C. (2012). On the trail of the glucocorticoid receptor: into the nucleus and back. Traffic, 13(3), 364-374.

Wang, S., Zhao, Z., Feng, X., Cheng, Z., Xiong, Z., Wang, T., Lin, J., Zhang, M., Hu, J., & Fan, Y. (2018). Melatonin activates Parkin translocation and rescues the impaired mitophagy activity of diabetic cardiomyopathy through Mst1 inhibition. Journal of Cellular and Molecular Medicine, 22(10), 5132-5144.

Wang, Z., Frederick, J., & Garabedian, M. J. (2002). Deciphering the Phosphorylation "Code" of the Glucocorticoid Receptor in Vivo 210. Journal of Biological Chemistry, 277(29), 26573-26580.

Xu, L., Hao, H., Hao, Y., Wei, G., Li, G., Ma, P., Xu, L., Ding, N., Ma, S., & Chen, A. F. (2019). Aberrant MFN2 transcription facilitates homocysteine-induced VSMCs proliferation via the increased binding of c-Myc to DNMT1 in atherosclerosis. Journal of Cellular and Molecular Medicine, 23(7), 4611-4626.

Yang, X., Ewald, E. R., Huo, Y., Tamashiro, K. L., Salvatori, R., Sawa, A., Wand, G. S., & Lee, R. S. (2012). Glucocorticoid-induced loss of DNA methylation in non-neuronal cells and potential involvement of DNMT1 in epigenetic regulation of FKBP5. Biochemical and Biophysical Research Communications, 420(3), 570-575.

Zgajnar, N. R., De Leo, S. A., Lotufo, C. M., Erlejman, A. G., Piwien-Pilipuk, G., & Galigniana, M. D. (2019). Biological actions of the Hsp90-binding immunophilins FKBP51 and FKBP52. Biomolecules, 9(2), 52.

Zhang, T.-Y., Keown, C. L., Wen, X., Li, J., Vousden, D. A., Anacker, C., Bhattacharyya, U., Ryan, R., Diorio, J., & O' Toole, N. (2018). Environmental enrichment increases transcriptional and epigenetic differentiation between mouse dorsal and ventral dentate gyrus. Nature Communications, 9(1), 1-11.

Zhang, Y., Leung, D. Y., Nordeen, S. K., & Goleva, E. (2009). Estrogen inhibits glucocorticoid action via protein phosphatase 5 (PP5)-mediated glucocorticoid receptor dephosphorylation. Journal of Biological Chemistry, 284(36), 24542-24552.

Zisapel, N., Tarrasch, R., & Laudon, M. (2005). The relationship between melatonin and cortisol rhythms: clinical implications of melatonin therapy. Drug Development Research, 65(3), 119-125.

국 문 초 록

신경세포에서 당질코르티코이드 유도성 미토콘드리아 기능 장애에 대한 멜라토닌의 방어 효과

서울대학교 대학원

수의학과 수의생명과학 전공

김 민 정

지도교수 한 호 재

당질코르티코이드와 멜라토닌은 일주기 리듬을 조절하며 신경 항상성을 유지하는 호르몬이다. 그러나, 스트레스로 인해 증가된 당질코르티코이드는 당질코르티코이드 수용체(GR)를 활성화시켜 미토파지 결함을 비롯한 미토콘드리아 기능 장애를 유발하여 신경 세포 사멸을 일으킨다. 반면에 멜라토닌은 당질코르티코이드에 의해 유발된 스트레스 매개성 신경 퇴행을 억제

한다. 따라서 이 연구는 멜라토닌이 당질코르티코이드에 의해 유발된 미토콘드리아 기능 장애 및 신경 퇴행에 방어 작용을 가지고 있는지 알아보기 위해 수행되었다. 먼저, 멜라토닌은 GR의 핵 내 이동을 막아 당질코르티코이드에 의해 억제된 NIX 매개 미토파지를 개선시켜 미토콘드리아 기능 장애에 기인한 신경 세포 사멸을 감소시켰다. 더 나아가 멜라토닌은 당질코르티코이드에 노출된 마우스의 인지 기능 장애를 개선시켰다. 더 나아가 멜라토닌은 GR의 핵 내 이동에 관여하는 단백질인 FKBP4의 발현을 선택적으로 억제하여 GR의 핵 내 이동을 감소시키는데 기인하였다. FKBP4 발현 억제는 멜라토닌 수용체 1(MT1) 의존성 경로를 통해 ERK의 인산화를 촉진시켜 *FKBP52* 프로모터의 DNMT1 매개 과메틸화에 의해 발생하였다. 결론적으로 멜라토닌이 당질코르티코이드에 의해 억제된 NIX 발현을 완화시켜 미토콘드리아 기능 장애와 세포 사멸을 감소시켰다. 또한, 멜라토닌이 DNMT1에 의한 FKBP4 하향조절을 통해 GR의 핵 내이동을 감소시켜 당질코르티코이드에 의한 미토파지 결함 및 신경 퇴행에 대한 방어 작용을 가지고 있음을 확인하였다.

주요어: 멜라토닌, 당질코르티코이드, 당질코르티코이드 수용체, 미토파지, 세포사멸, FKBP4

학번: 2020-27673